Pipeline development

Collaboration with Bicycle Therapeutics

Poster presented at TIDES 2023

Potent anti-tumor activity of a Lead-212 labelled MT1-MMP targeting Bicycle Radionuclide Conjugate™

Gemma E. Mudd[1], Amal Saidi[3], Anusha Regupathy[1], Tania A. Stallons[4], Amy Wong[4], Paul Beswick[1], Katerine van Rietschoten[1], Kevin McDonnell[2], Julien Torgue[4], Michael J. Skynner[1], Nicholas Keen[2], Kevin Lee[1]

[1]BicycleTx Limited, Portway Building, Granta Park, Cambridge, CB21 6GS, UK
[2]Bicycle Therapeutics, Inc. 35 Cambridgepark Drive, Cambridge, MA, 02140 USA
[3]Orano Med SAS, Courbevoie, France
[4]Orano Med LLC, Plano, Texas, United States of America

Abstract

^{212}Pb-BCY20603 is a Bicycle Radionuclide Conjugate™ (BRC™), which comprises a bicyclic peptide that binds with high affinity to the tumor antigen MT1-MMP and a chelate of Lead-212, a potent alpha particle emitting radioisotope. ^{212}Pb-BCY20603 shows tumor targeting in rodent tumor xenograft studies, with radioactivity levels of >45% injected dose per gram (ID/g) 24 hours post injection. It is well tolerated and in rodent efficacy studies, shows potent anti-tumor activity after a single dose of 5 µCi. Complete tumor regressions were seen after 3 dosing cycles of 10 µCi, given two weeks apart, with no tumor regrowth at the end of the 100-day study.

Introduction

- **Targeted alpha therapy (TAT)** allows selective delivery of potent, alpha particle emitting radioisotopes to tumors through conjugation of the payload to a tumor antigen targeting molecule
- **Bicyclic peptides (*Bicycles*)** are an ideal modality for radioisotope delivery: they can achieve high affinity and selective binding to the desired tumor target, and their small size (vs biologics) allows good tumor penetration for effective payload delivery.[1,2]
- **Membrane type 1 matrix metalloproteinase (MT1-MMP / MMP-14)** is an extracellular membrane bound protein which is highly expressed in a range of cancers, including breast, non-small cell lung and gastric cancer, but has relatively low expression in healthy tissue. These properties make it an ideal target for selective radioisotope delivery. [3]
- **Lead-212** is an alpha particle emitting radioisotope. It has a decay half-life of 11 hours, which is well suited for small molecules and peptides that have short circulating half-lives.
- **Orano Med** generate Lead-212 *via* a chemical production process that is robust and economical.[4]

Bicycle Radionuclide Conjugate™ (BRC™) ^{212}Pb-BCY20603

(A) MT1-MMP targeting *Bicycle*
- **High affinity** (5 nM) binding to tumor antigen MT1-MMP
- Allows **precision** targeting of BRC™ to tumor cells

(B) Lead-212
- **Potent radioisotope payload** that causes double strand DNA breaks through a single alpha particle emission

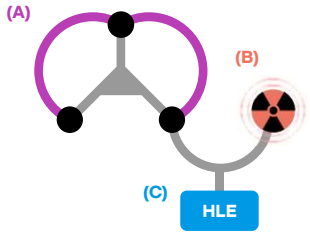

(C) Half-life extending moiety
- Reversible albumin binding motif
- Prolongs circulating half-life of conjugate[5]

Results

^{212}Pb-BCY20603 shows activity levels of >45% ID/g 24 hours post injection

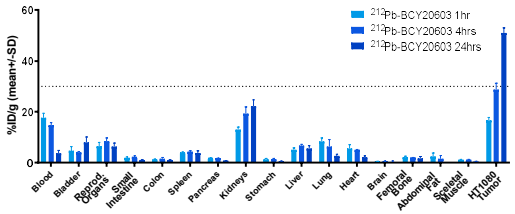

Figure 1: ***In vivo*** **distribution of ^{212}Pb-BCY20603 in athymic nude female mice carrying subcutaneous HT1080 tumors: 10µCi of drug was administered and organs were collected from 5 mice per timepoint: 1 hour, 4 hours and 24 hours post injection. The tissue uptake is expressed as %ID per gram (n=5). The background was automatically subtracted from the counts. A 5µl standard is used for decay correction. %ID/g was calculated for each organ collected.**

^{212}Pb-BCY20603 shows a favorable biodistribution profile, with mean tumor levels of 16, 29 and 51% ID/g at 1, 4 and 24 hours respectively and a tumor to kidney ratio >1. (Fig. 1). In comparison, a Lead-212 labelled MT1-MMP targeting antibody (^{212}Pb-MT1-MMP-mAb) shows high radioactivity levels in spleen and lung, with very low activity levels in the tumor at all timepoints (Fig. 2). These data highlight the potential suitability of *Bicycles* for targeted delivery of Lead-212 to tumors and their advantages over large biologics.

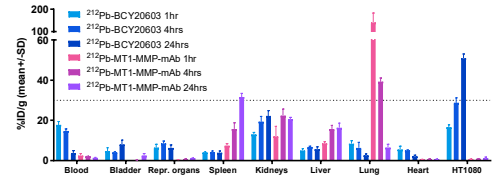

Figure 2: Comparison of *in vivo* distribution of ^{212}Pb-BCY20603 and a ^{212}Pb-MT1-MMP-mAb. Experimental setup as described for Figure 1.

^{212}Pb-BCY20603 is well tolerated up to 40µCi as a single dose

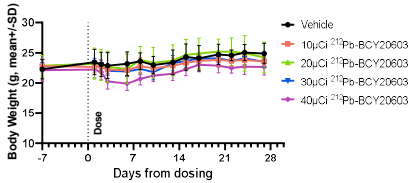

Figure 3: ^{212}Pb-BCY20603 dose range finding (DRF) study. Compound was given as a single IV dose at 10, 20, 30 or 40 µCi to Athymic nude mice. Animals underwent daily observations and 3x per week weighing. Animals were sacrificed at 4 weeks or when termination criteria were met. N = 5 animals per group.

^{212}Pb-BCY20603 was well tolerated as a single dose up to 40 µCi. No body weight loss was seen in groups treated with 10, 20 and 30 µCi. Although slight body weight loss was observed following dosing at 40 µCi, animals recovered quickly. No significant changes were observed in hematology readout when compared to vehicle treated mice (Student's t-test p>0.05, data not shown). As a comparison, the maximum tolerated dose of peptide-based somatostatin receptor targeting TAT agent ^{212}Pb-DOTAMTATE was found to be 20-40 µCi.[6]

^{212}Pb-BCY20603 shows rapid and homogeneous tumor microdistribution

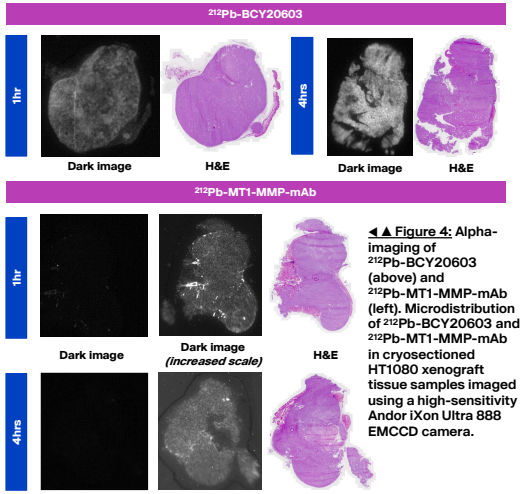

◀▲ Figure 4: Alpha-imaging of ^{212}Pb-BCY20603 (above) and ^{212}Pb-MT1-MMP-mAb (left). Microdistribution of ^{212}Pb-BCY20603 and ^{212}Pb-MT1-MMP-mAb in cryosectioned HT1080 xenograft tissue samples imaged using a high-sensitivity Andor iXon Ultra 888 EMCCD camera.

Alpha imaging of tumor sections at 1- and 4- hours post injection shows that ^{212}Pb-BCY20603 is rapidly accumulated in the tumor with homogeneous distribution. In comparison, a Lead-212 labelled MT1-MMP targeting antibody shows very low, heterogeneous uptake in the tumor at the same timepoints.

^{212}Pb-BCY20603 shows potent anti-tumor activity in an MT1-MMP expressing xenograft model

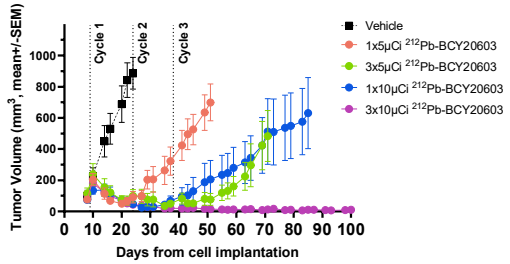

Figure 5: Anti-tumor activity of ^{212}Pb-BCY20603 in HT1080 tumor carrying athymic nude mice. Groups were treated with ^{212}Pb-BCY20603 at doses of 1x5 µCi, 1x10 µCi, 3x5 µCi or 3x10 µCi (dosing cycles 2 weeks apart). N = 8-10 animals per group.

In an *in vivo* efficacy study in mice, ^{212}Pb-BCY20603 showed potent anti-tumor activity. Tumor shrinkage was seen in groups treated with ^{212}Pb-BCY20603 at 1x5 µCi, 1x10 µCi, and 3x5 µCi (2-week dosing intervals). Animals dosed with 3x10 µCi showed complete tumor regressions and 6/10 animals were tumor free or regressing at the end of the 100-day study.

Administration of ^{212}Pb-BCY20603 led to increased survival at all doses tested

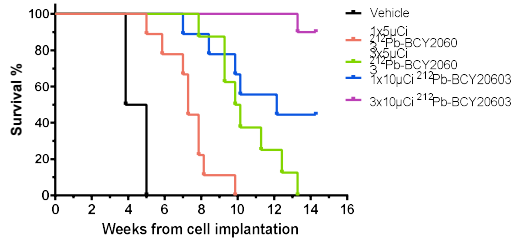

Figure 6: Survival plot of Athymic nude mice carrying HT1080 tumors and treated with 1x5 µCi, 1x10 µCi, 3x5 µCi or 3x10 µCi ^{212}Pb-BCY20603 (2- week dosing intervals).

▶ Table 1: Median survival of animals in each dosing group

Dose	Median survival (weeks)
Vehicle	4.4
1x5 µCi	7.2
1x10 µCi	10.0
3x5 µCi	12.1
3x10 µCi	Not reached

Median survival was increased for each dosing group. 90% survival was seen for the highest dose group which were treated with 3 cycles of 10 µCi ^{212}Pb-BCY20603 every two weeks.

Conclusions

- ^{212}Pb-BCY20603 binds to MT1-MMP with high affinity
- Tumor targeting of ^{212}Pb-BCY20603 has been demonstrated in mice, with activity levels >45% ID/g after 24 hours and a tumor to kidney ratio of >1.
- ^{212}Pb-BCY20603 is well tolerated up to 40µCi in single dose mouse DRF studies and shows potent anti-tumor activity
- Complete tumor regressions were seen in mouse xenograft groups dosed with 3x10 µCi, dosing every 2 weeks
- To our knowledge, this is the first example of anti-tumor activity demonstrated with an MT1-MMP targeting radio conjugate
- We believe these data indicate that *Bicycles* are well suited for selective delivery of radionuclide payloads to tumors

References

[1] Bennett, G. et al. MMAE Delivery Using the Bicycle Toxin Conjugate BT5528. Molecular Cancer Therapeutics 19, 1385, doi:10.1158/1535-7163.MCT-19-1092 (2020).
[2] Rigby, M. et al. BT8009; A Nectin-4 Targeting Bicycle Toxin Conjugate for Treatment of Solid Tumors. Molecular Cancer Therapeutics 21, 1747-1756, (2022).
[3] Eder, M. et al. Bicyclic Peptides as a New Modality for Imaging and Targeting of Proteins Overexpressed by Tumors. Cancer Research 79, 841, (2019).
[4] Torgue, J., Maquaire, P., Young, J., Andreoletti, G. & Bourdet, P. Method and apparatus for the production of lead 212 for medical use. US20150170776 (2015).
[5] Lau, J. *et al.* Bench to Bedside: Albumin Binders for Improved Cancer Radioligand Therapies. Bioconjugate Chemistry 30, 487-502, (2019).
[6] Stallons, T. A. R., et al.. Preclinical Investigation of 212Pb-DOTAMTATE for Peptide Receptor Radionuclide Therapy in a Neuroendocrine Tumor Model. Molecular Cancer Therapeutics 18, 1012-1021, (2019).

Bicycle Therapeutics, Inc.
35 Cambridgepark Drive
Suite 350
Cambridge, MA 02140

BicycleTx Limited
Portway Building
Granta Park
Cambridge CB21 6GP

Collaboration with Nordic Nanovector

PLOS ONE

RESEARCH ARTICLE

Targeted alpha therapy for chronic lymphocytic leukaemia and non-Hodgkin's lymphoma with the anti-CD37 radioimmunoconjugate ^{212}Pb-NNV003

Astri Fjelde Maaland[1,2☯]*, Amal Saidi[3☯], Julien Torgue[4], Helen Heyerdahl[1], Tania A. Rozgaja Stallons[4], Arne Kolstad[5,6], Jostein Dahle[1]

1 Nordic Nanovector ASA, Oslo, Norway, **2** Institute of Clinical Medicine, University of Oslo, Oslo, Norway, **3** Orano Med SAS, Courbevoie, France, **4** Orano Med LLC, Plano, Texas, United States of America, **5** Department of Oncology, Oslo University Hospital, Radiumhospitalet, Oslo, Norway, **6** KG Jebsen Center for Cancer Immunotherapy, Institute of Clinical Medicine, University of Oslo, Oslo, Norway

☯ These authors contributed equally to this work.
* astri.maaland@gmail.com

Citation: Maaland AF, Saidi A, Torgue J, Heyerdahl H, Stallons TAR, Kolstad A, et al. (2020) Targeted alpha therapy for chronic lymphocytic leukaemia and non-Hodgkin's lymphoma with the anti-CD37 radioimmunoconjugate ^{212}Pb-NNV003. PLoS ONE 15(3): e0230526. https://doi.org/10.1371/journal.pone.0230526

Editor: Jonathan Engle, University of Wisconsin, UNITED STATES

Received: November 6, 2019

Accepted: March 2, 2020

Published: March 18, 2020

Data Availability Statement: All relevant data are within the manuscript and its Supporting Information files.

Funding: This study was partially funded by the Norwegian Research Council, grant number 25690, and by Nordic Nanovector ASA and Orano Med. The funders provided support in the form of salaries for authors AFM, AS, JT, HH, TARS and JD, but did not have any additional role in the study design, data collection and analysis, decision to

Abstract

Relapse of chronic lymphocytic leukaemia and non-Hodgkin's lymphoma after standard of care treatment is common and new therapies are needed. The targeted alpha therapy with ^{212}Pb-NNV003 presented in this study combines cytotoxic α-particles from ^{212}Pb, with the anti-CD37 antibody NNV003, targeting B-cell malignancies. The goal of this study was to explore ^{212}Pb-NNV003 for treatment of CD37 positive chronic lymphocytic leukaemia and non-Hodgkin's lymphoma in preclinical mouse models.An anti-proliferative effect of ^{212}Pb-NNV003 was observed in both chronic lymphocytic leukaemia (MEC-2) and Burkitt's lymphoma (Daudi) cells *in vitro*. In biodistribution experiments, accumulation of ^{212}Pb-NNV003 was 23%ID/g and 16%ID/g in Daudi and MEC-2 tumours 24 h post injection. In two intravenous animal models 90% of the mice treated with a single injection of ^{212}Pb-NNV003 were alive 28 weeks post cell injection. Median survival times of control groups were 5–9 weeks. There was no significant difference between different specific activities of ^{212}Pb-NNV003 with regards to therapeutic effect or toxicity. For therapeutically effective activities, a transient haematological toxicity was observed. This study shows that ^{212}Pb-NNV003 is effective and safe in preclinical models of CD37 positive chronic lymphocytic leukaemia and non-Hodgkin's lymphoma, warranting future clinical testing.

Introduction

In the USA, chronic lymphocytic leukaemia (CLL) and non-Hodgkin's lymphoma (NHL) account for 1.2% and 4.3% of all new cancer incidence, with a combined estimated number of new cases of approximately 95,000 in 2019 [1, 2]. The standard of care for CLL is chemotherapy in combination with anti-CD20 antibodies. However, small molecular inhibitors are

publish, or preparation of the manuscript. The specific roles of these authors are articulated in the 'author contributions' section. No additional external funding received for this study.

Competing interests: I have read the journal's policy and the authors of this manuscript have the following competing interests: JD and HH are employees and shareholders of Nordic Nanovector ASA. AFM is a PhD student employed by Nordic Nanovector ASA, funded by the Norwegian Research Council. AK is a member of the Scientific Advisory Board of Nordic Nanovector ASA. AS is employed by Orano Med SAS, TARS and JT are employed by Orano Med LLC. Patents: PCT/EP2011/051231 (Radioimmunoconjugates and uses thereof), PCT/EP2014/061824 (Method for upregulating antigen expression), PCT/EP2017/073336 (Treatment of non-Hodgkin lymphoma using lilotomab and 177Lu-lilotomab satetraxetan), PCT/EP2018/082065 (Radioimmunoconjugates in combination with other drugs as treatment against NHL), EP2854870B1 (Method and apparatus for the production of lead 212 for medical use), EP3174068B1 (New method and apparatus for the production of high purity radionuclides). This does not alter our adherence to PLOS ONE policies on sharing data and materials.

emerging as new therapies. While these regimens are initially effective in inducing responses, most patients eventually relapse and become refractory to further treatments [3–5]. NHL comprises a more heterogeneous group of diseases where treatment varies between subtypes. The backbone for most patients is chemotherapy combined with anti-CD20 antibodies. Indolent types of NHL are commonly diagnosed at advanced stage and thus incurable, but median survival is expected to be 15–20 years [6]. More aggressive subtypes of NHL are curable with intensive therapies, but patients who experience relapse often have a dismal outcome [7]. Both for CLL and NHL, new therapies with different mechanisms of actions and targets are needed.

In this study we explore a novel strategy, a targeted alpha therapy (TAT). We have conjugated the IgG1 chimeric antibody NNV003 with the chelator TCMC and labelled it with the alpha-particle generating radionuclide ^{212}Pb (^{212}Pb-NNV003). NNV003 binds with high affinity to CD37 and has been shown to internalise in some cell lines and induce antibody-dependent cellular phagocytosis and antibody-dependent cellular cytotoxicity [8]. CD37 is a glycosylated transmembrane protein, which has emerged as a therapeutic target in the recent years. It is highly and selectively expressed by B-lymphocytes and B-cell malignancies [9]. There are currently three CD37 targeting therapies in clinical development [10–13]. One of these compounds, ^{177}Lu-lilotomab satetraxetan (Betalutin®), applies the β-emitter lutetium-177 as the cytotoxic payload, and is currently in clinical phase 2b for patients with relapsed follicular lymphoma (NCT01796171) [13]. Unlike NHL, where enlarged lymph nodes and tumours dominate the clinical picture, CLL more often presents as a disseminated leukemic disease. In theory, it would be more advantageous to use an α-emitter as the cytotoxic payload in CLL. Due to the α-particles' short range of 50–100 μm, the radiation will be more localised to target cells than β-particles that have a range of 0.05–12 mm. The α-particles' high LET of 100 keV/μm creates irreparable DNA double strand breaks. Consequently, only 2–3 α-particles are needed to kill a single cell, compared to 100–1000 low LET β-particles [14]. ^{212}Pb has two alternative decay pathways through α-emitting daughters, ^{212}Bi or ^{212}Po, and can therefore be used as an *in vivo* generator of α-particles [15].

The anti-tumour efficacy of ^{212}Pb has been demonstrated in preclinical studies; in several animal models of peritoneal cancer [16–22], prostate cancer, melanoma, pancreatic cancer and breast cancer [23–26]. It has also been applied in a pre-targeting setting [27, 28]. Recently, a phase 1 trial with ^{212}Pb-TCMC-trastuzumab documented safety and feasibility in patients with human HER2 expressing malignancies [29]. Furthermore, a phase 1 study of ^{212}Pb-DOTAMTATE for treatment of neuroendocrine tumours has been initiated (NCT03466216). In our study, we have investigated the *in vitro* cytotoxic effect of ^{212}Pb-NNV003 in a CLL and a Burkitt's lymphoma cell line. The *in vivo* tumour targeting of the TAT was studied in subcutaneous xenograft models. Two different disseminated models of CLL and NHL were used to evaluate the *in vivo* anti-tumour efficacy and toxicity of ^{212}Pb-NNV003.

Materials and methods

Ethics statement–animal research

All studies were conducted under the approval of the institutional IACUC committee, Orano Med Institutional Animal Care and Use Committee, ethical approval number IAC-PR-006. Mice were kept under pathogen-free condition in a 12-hour light/dark cycle, with ad libitum access to food and water. Temperature, humidity and air-flow was continuously monitored. The cages contained enrichments and the bedding was changed once a week. Animal health was monitored by trained staff. The mice were euthanised by cervical dislocation when humane end point was reached. ARRIVE guidelines were followed (S2 File). See Supplementary S1 File and S1 Table for more information.

Labelling antibodies with ^{212}Pb

NNV003 and cetuximab (binding to EGFR, used as unspecific control, Merck KGaA, Germany) were conjugated with a customised bifunctional version of TCMC (1,4,7,10-Tetrakis(carbamoyl-methyl)-1,4,7,10-tetraazacyclododecane, Macrocyclics, USA), using an enzymatic procedure based on a process described by Jeger [30] and Dennler [31] resulting in up to two TCMC molecules conjugated to a specific amino acid in the Fc part of the antibody. An over 99.9% radiochemically pure ^{212}Pb was eluted with 0.4 M ammonium acetate from a ^{224}Ra generator (Orano Med LLC, USA). TCMC-NNV003 and TCMC-cetuximab in 150 mM ammonium acetate were added to purified ^{212}Pb at ratios of 3.7, 37 or 370 MBq/mg and incubated at 37˚C for 10 min with shaking at 300 rpm. ITLC was used to confirm a chelation > 95%. Samples were diluted in 0.9% NaCl prior to injection. Specific activities (SA) used: 37 MBq/mg (biodistribution and acute toxicity studies), 370 MBq/mg (cytotoxicity assay) and 3.7–370 MBq/mg (therapy studies). The immunoreactivity (IRF) of ^{212}Pb-NNV003 was measured as previously described [8].

Cell lines

The human CLL cell line MEC-2 (Creative Bioarray, USA) and the Burkitt's lymphoma cell line Daudi (ATCC, USA) were cultured in IMDM and RPMI medium. Media were supplemented with 10% heat inactivated fetal bovine serum and 1% Penicillin-Streptomycin (ATCC, USA).

In vitro studies

MEC-2 and Daudi cells (1x10^6) were fixed in 1% formaldehyde for 15 min at 4˚C, stained with 5 μL Alexa Fluor® 647 mouse anti-human CD37 (Clone M-B371, BD Bioscience, USA) for 30 min on ice in the dark and analysed in a Guava easyCyte 8HT (Millipore, USA).

MEC-2 and Daudi cells were plated in 96 well-plates with 5000 cells/well. ^{212}Pb-NNV003 or ^{212}Pb-cetuximab was added to the cells at final concentrations of 57.8 Bq/ml to 14.8 kBq/ml (n = 8 wells per concentration). The cells were incubated for 5 h before washing. After resuspending in fresh medium, the cells were kept in culture for 6 more days. The CyQUANT™ NF Cell Proliferation Assay Kit (Thermo Fisher Scientific, USA) was used to measure cell proliferation.

Biodistribution

10x10^6 Daudi or 2.5x10^6 MEC-2 cells were injected subcutaneously (s.c) in the flank of 15 female CB17 SCID mice (CB17/Icr-*Prkdc*^{scid}/IcrIcoCrl, Charles River Laboratories, USA) or 24 female R2G2 mice (B6;129-*Rag2*^{tm1Fwa}*Il2rg*^{tm1Rsky}/DwlHsd, Envigo, USA). When tumours reached a volume of 200–300 mm^3, 200 μg murine IgG2a (M7769-5MG, Sigma Aldrich, USA) was injected intraperitoneally (i.p.). Next day, 370 kBq ^{212}Pb-NNV003 was injected intravenously (i.v.). Mice were euthanised at predetermined time-points: 1 h (n = 5 CB17 SCID, n = 10 R2G2), 6 h (n = 5 CB17 SCID, n = 4 R2G2) and 24 h (n = 5 CB17 SCID, n = 10 R2G2). Organs and tumours were harvested, weighted and the activity was measured by a calibrated gamma counter (Wizard2, Perkin Elmer, USA). The background was subtracted from the measurements and values were decay corrected. Percent injected dose/g (%ID/g) was calculated for each tissue.

Radiation dosimetry

The biodistribution data from the two s.c. models was used to calculate the absorbed radiation doses from ^{212}Pb-NNV003, performed by Rapid (Maryland, USA). Time-integrated activity coefficients were obtained by the trapezoidal method as the data could not be exponentially fitted. Physical decay was used to extrapolate after the last time point.

Toxicity studies of ^{212}Pb-NNV003

Female CB17 SCID mice (30 total, n = 5 per group) were injected i.v. with ^{212}Pb-NNV003 or PBS. Female R2G2 mice (29 total) were injected i.v. with ^{212}Pb-NNV003 (n = 5 per group), 0.9% NaCl or ^{212}Pb-cetuximab (n = 3 per group), to ensure similar tolerability of the two TATs. 200 μg murine IgG2a was injected i.p. one day before TAT injection. The mice were weighed three times a week and observed daily for clinical signs of radiotoxicity. Mice were euthanised when termination criteria were met (see Termination criteria section). Histopathological examinations were performed by Comparative Bioscience Inc (USA) on organs collected from R2G2 mice.

In both therapy models described below the concentration of platelets, red blood cells and white blood cells were monitored (see Haematological toxicity section).

Therapy studies

To mimic disseminated CLL disease, 68 female R2G2 mice were i.v. injected with $2.5x10^6$ MEC-2 cells two days prior to treatment with ^{212}Pb-NNV003 (370 MBq/mg), ^{212}Pb-cetuximab (370 MBq/mg), NNV003-TCMC or 0.9% NaCl (n = 10). This model was also used to test different SAs of ^{212}Pb-NNV003. 70 R2G2 mice were i.v. injected with MEC-2 cells, and received 370 kBq ^{212}Pb-NNV003 (3.7, 37 or 370 MBq/mg), 370 kBq ^{212}Pb-cetuximab (3.7 MBq/mg), NNV003-TCMC or 0.9% NaCl (n = 10 per group).

67 female CB17 SCID mice were i.v. injected with $10x10^6$ Daudi cells two days before treatment with ^{212}Pb-NNV003 (370 MBq/mg), ^{212}Pb-cetuximab, NNV003-TCMC or 0.9% NaCl (n = 12 for 280 kBq ^{212}Pb-NNV003 and n = 11 for the other groups). In all studies, animals received 200 μg murine IgG2a i.p. the day before treatment. The mice were checked daily for clinical symptoms and body weights were monitored. They were euthanised when termination criteria were met (see Termination criteria section). Statistical analysis performed as described in Statistics section.

Haematological toxicity

In both therapy models in the study, the concentration of platelets, red blood cells and white blood cells were monitored. 100 μL blood was collected prior to treatment and every two weeks thereafter from the retro-orbital sinus. The cell concentrations were determined using Vetscan HM5 hematology analyzer (Abaxis, USA). Animals received 300 μL 0.9% NaCl i.p. after blood collection. Statistical analysis was performed as described in the Statistics section.

Termination criteria

Animals were euthanised by cervical dislocation when a combination of following humane end-points occurred: weight loss $>$ 15% over two consecutive days, lack of grooming over 5 days, weakness over 3 days, reduced motility, paralysis, palpable abdominal tumour $>$ 1000 mm^3, hunched back, severe anaemia and diarrhoea.

Statistics

All statistical analysis were done in GraphPad Prism 7.00 (GraphPad Software, USA). Log rank tests were performed for pairwise comparisons of treatment groups in the therapy studies. The Holm-Sidak method for multiple comparisons correction was used, with a significance level of $\alpha = 0.05$. The platelet counts of the ^{212}Pb-NNV003 treated mice were compared with the NaCl treated mice by one-way ANOVA followed by the Dunnett's multiple comparison test with significance level of $\alpha = 0.05$.

Results

Immunoreactivity of ^{212}Pb-NNV003

The IRF of ^{212}Pb-NNV003 was measured after initiation of the studies and was found to be around 57%. This suboptimal binding was due to radiation induced oxidation of the antibody after labelling and not the conjugation method. The addition of ascorbic acid during labelling restored the binding of ^{212}Pb-NNV003 to the cells to approximately 80%, which is normally obtained with NNV003 labelled with lutetium-177 [8].

CD37 expression and cytotoxicity of ^{212}Pb-NNV003

CD37 expression was approximately 20 times higher in Daudi cells than MEC-2 cells (Fig 1A). ^{212}Pb-NNV003 had a dose dependent anti-proliferative effect on both cell lines, while ^{212}Pb-cetuximab only had modest effect at the highest concentrations (Fig 1B). Daudi cells appeared more sensitive than MEC-2 cells. The experiment was repeated, and the trend was confirmed (S2 Fig).

Biodistribution and dosimetry of ^{212}Pb-NNV003

In each animal study the mice were predosed with murine IgG2a before TAT injection to decrease the binding of ^{212}Pb-NNV003 to murine Fc receptors and thus prevent clearance of antibody to spleen and liver in immune deficient mice with low amounts of endogenous antibodies [32]. Murine IgG2a binds with a similar affinity as human IgG1 to murine Fc receptors [33, 34]. A biodistribution performed in CB17 SCID mice revealed significant decrease in ^{212}Pb-NNV003 uptake in spleen, kidneys and liver (S3A Fig). In immune competent Balb/c mice, however, the biodistribution was not altered by the predosing with IgG2a (S3B Fig).

^{212}Pb-NNV003 was rapidly taken up in blood rich organs and thymus. Accumulation in tumour was slower but reached approximately 23%ID/g in Daudi tumours and 16%ID/g in MEC-2 tumours after 24 h (Fig 2A and 2B). The lack of redistribution of the radionuclide after initial uptake in organs indicates *in vivo* stability of ^{212}Pb-NNV003.

The tissue absorbed doses from the TAT is presented in Fig 3. Alpha radiation contributes most to the total absorbed dose, which was highest in blood rich organs and in the tumours.

Acute toxicity of ^{212}Pb-NNV003

The CB17 SCID mice that reached termination criteria were euthanised because of acute radiation toxicity. One mouse treated with 740 kBq was found dead in the cage, assumed dead of radiation toxicity. No R2G2 mice reached termination criteria. Remaining CB17 SCID and the R2G2 mice were euthanised at the end of the studies, 29 (CB17 SCID) or 33 (R2G2) days after TAT injection.

1480 kBq ^{212}Pb-NNV003 was too toxic for the CB17 SCID mice, and within a week after injection, all mice had been euthanised due to weight loss (Fig 4A and 4B). Doses of 370–740 kBq ^{212}Pb-NNV003 also caused radiotoxicity with weight loss and 40–60% of the mice had to be euthanised within three weeks post injection. However, the lowest dose, 185 kBq, was well tolerated. CB17 SCID mice are known to have low tolerance to ionising radiation, due to a deficiency in the DNA double strand break repair mechanism [35]. Therefore, R2G2 mice were used for the MEC-2 model since they do not possess the SCID mutation and are therefore less sensitive to radiation. Indeed, doses of 185–555 kBq of ^{212}Pb-NNV003 and 555 kBq of ^{212}Pb-cetuximab could be administered in R2G2 mice without mortality, with only a mild and reversible initial weight loss (Fig 4C and 4D). Histopathological examination of the treated R2G2 mice showed no signs of radiation induced damage. From these results, the highest non-

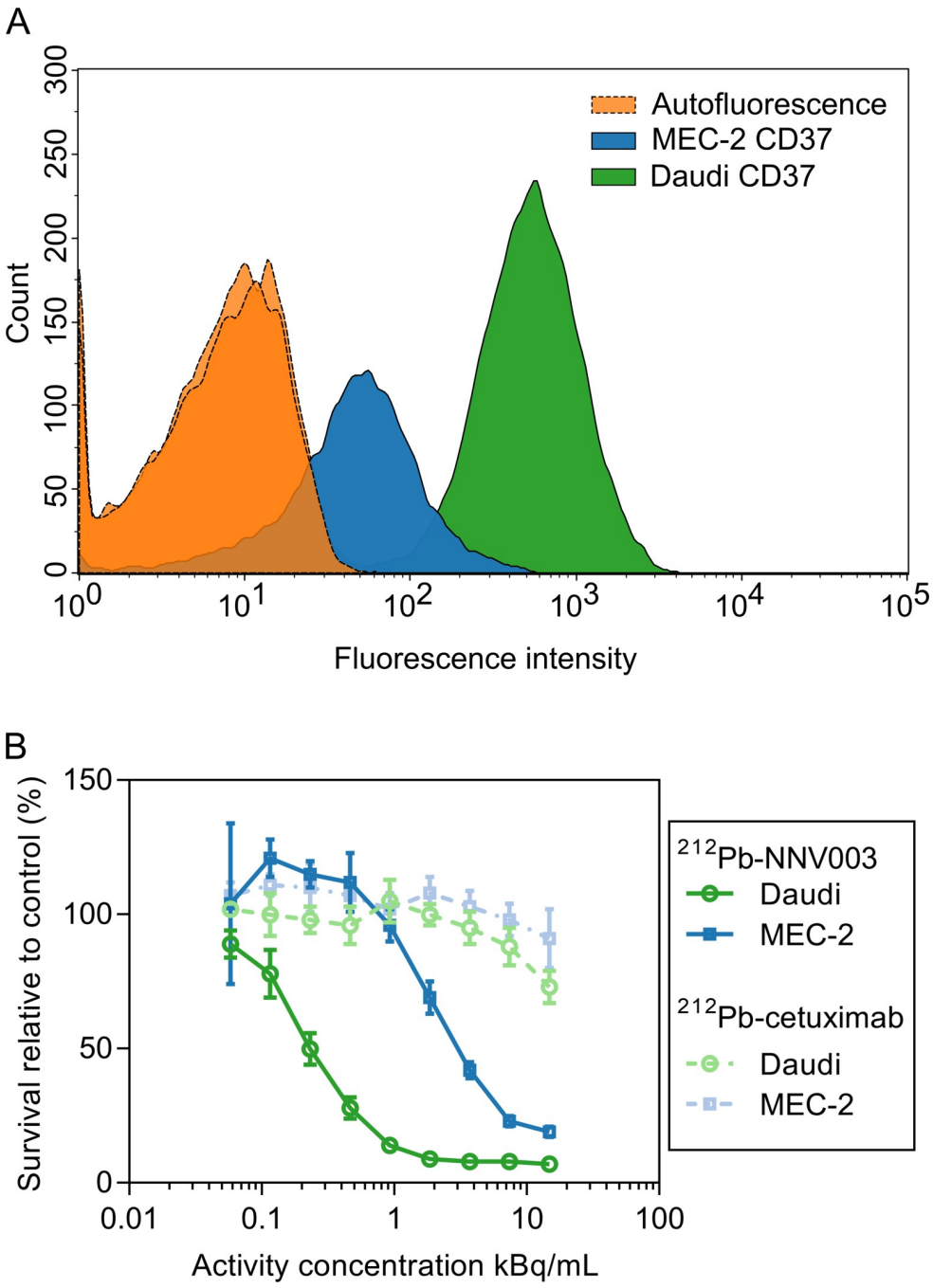

Fig 1. CD37 expression and cytotoxic effect of ^{212}Pb-NNV003. (A) Flow cytometry histograms of cells only and cells incubated with 5 μl Alexa Fluor® 647 anti-human CD37. (B) Proliferation of Daudi and MEC-2 cells treated with ^{212}Pb-NNV003 or ^{212}Pb-cetuximab. Data represented as average of n = 8 replicates and error bars = SD.

https://doi.org/10.1371/journal.pone.0230526.g001

severely toxic doses (HNSTD) were established: 185 kBq in CB17 SCID mice and 555 kBq in R2G2 mice, and the following ^{212}Pb-NNV003 doses were chosen for therapy studies: 90, 185 and 280 kBq (CB17 SCID) and 185, 370, 555 and 740 kBq (R2G2). The two additional doses of 280 kBq (CB17 SCID) and 740 kBq (R2G2) that were not tested in the acute toxicity studies were included to test the range of the therapeutic window.

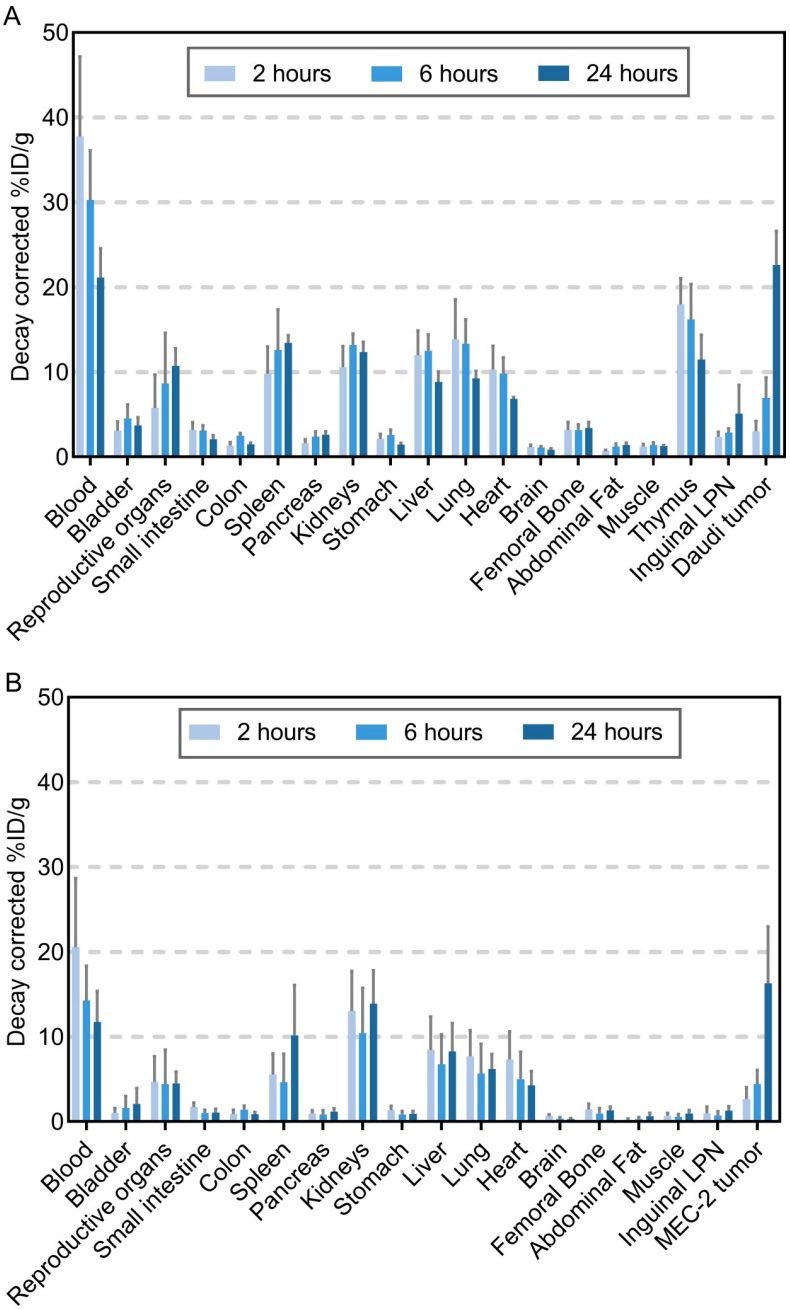

Fig 2. Biodistribution of ^{212}Pb-NNV003. %ID/g of ^{212}Pb-NNV003 in tissues of (A) CB17 SCID mice with Daudi s.c. xenografts (n = 5 per time point) and (B) R2G2 mice with MEC-2 s.c. xenografts (n = 4 at 6 h, n = 10 at 2 and 24 h). Data presented as averages with error bars = SD, LPN = Lymph Node.

https://doi.org/10.1371/journal.pone.0230526.g002

Anti-tumour effect of ^{212}Pb-NNV003

In the disseminated model of NHL, the injected Daudi cells infiltrated the bone marrow of the mice causing hind leg paralysis. The CLL model had a more aggressive profile, where the MEC-2 cells mostly infiltrated abdominal tissues, forming tumours in and around ovaries, kidneys, liver and spleen, and therefore represented a more difficult model to treat than the NHL model. Because of the aggressive profile, R2G2 mice were used for the MEC-2 model,

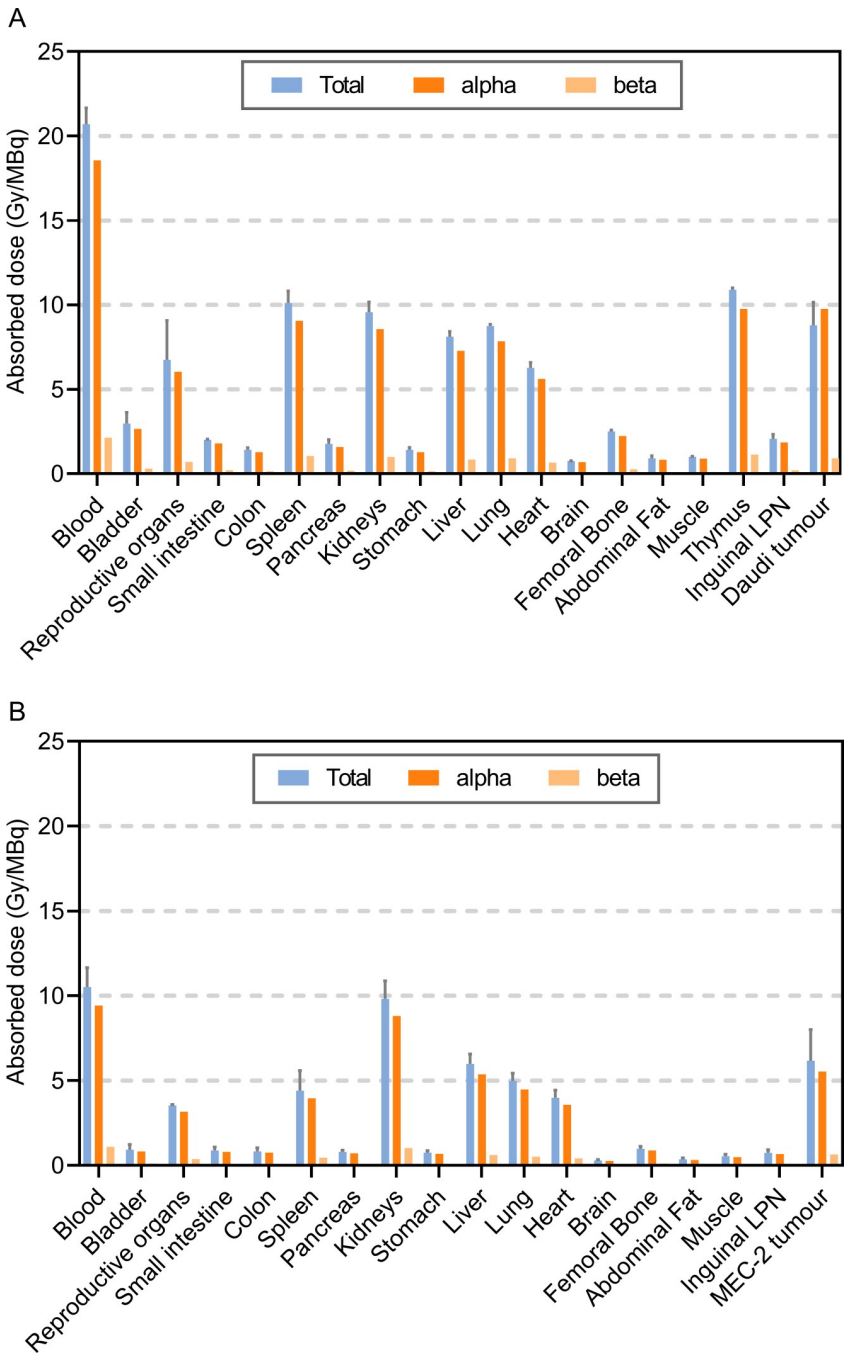

Fig 3. Dosimetry of ^{212}Pb-NNV003. Absorbed radiation dose (Gy/MBq) to tissues of (A) CB17 SCID mice with Daudi s.c. xenografts (n = 5 per time point) and (B) R2G2 mice with MEC-2 s.c. xenografts (n = 4 at 6 h, n = 10 at 2 and 24 h). Error bars = SD of total absorbed radiation dose.

https://doi.org/10.1371/journal.pone.0230526.g003

permitting treatment with a higher dose than is possible in CB17 SCID mice. The SCID mutation impairs the DNA double strand break repair pathway, making the mouse strain inherently sensitive to radiation [35]. The mice that reached termination criteria were euthanised because of tumour infiltration or acute radiation toxicity (2 mice treated with 370 and 740 kBq ^{212}Pb-NNV003). Three R2G2 mice, treated with either 185 kBq ^{212}Pb-NNV003, 370 kBq ^{212}Pb-

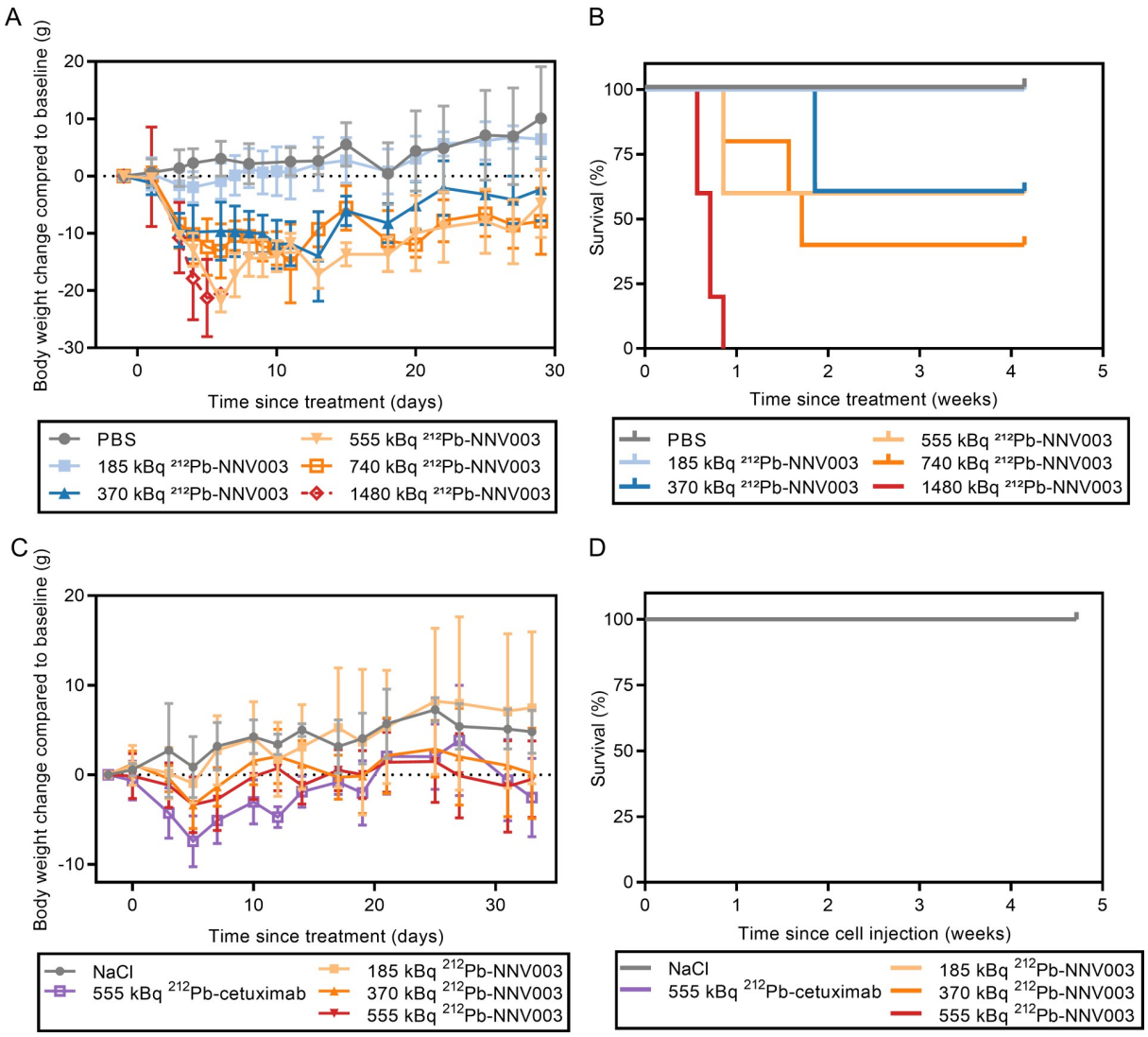

Fig 4. Acute toxicity of ^{212}Pb-NNV003. CB17 SCIDs were injected i.v. with increasing dose of ^{212}Pb-NNV003 or PBS. (A) Body weights (average of n = 5, error bars = SD) and (B) survival of the mice. R2G2 mice were injected with increasing dose of ^{212}Pb-NNV003 (n = 5), ^{212}Pb-cetuximab or NaCl (n = 3). (C) Body weight (average with error bars = SD) and (D) survival of the mice (overlapping curves).

https://doi.org/10.1371/journal.pone.0230526.g004

cetuximab or 10 μg NNV003, and one CB17 SCID mouse treated with 185 kBq ^{212}Pb-NNV003 were found dead in the cage and their cause of death was presumably related to tumour infiltration. The remaining mice were euthanised at the end of the study, 201 (Fig 5A), 197 (Fig 5B) or 150 (Fig 5C) days after cell injection.

In both models, a single injection of ^{212}Pb-NNV003 significantly prolonged median survival compared to controls (Fig 5A and 5B). At study termination 28 weeks post cell injection, 67–91% of the Daudi injected CB17 SCID mice and 30–90% of the MEC-2 injected R2G2 mice treated with ^{212}Pb-NNV003 were still alive. In the MEC-2 model, 555 kBq unspecific ^{212}Pb-cetuximab showed an anti-tumour effect comparable to the effect of 185 kBq ^{212}Pb-NNV003 (Fig 5B). There was a dose-dependent response to doses of 370 to 740 kBq ^{212}Pb-NNV003, which were more effective than ^{212}Pb-cetuximab, but only the 555 kBq dose of ^{212}Pb-NNV003 was statistically superior.

A single i.v. injection of 370 kBq ^{212}Pb-NNV003, with SA between 3.7 and 370 MBq/mg, improved survival of R2G2 mice i.v. injected with MEC-2 cells, compared to controls (Fig 5C). 60–90% of the R2G2 mice treated with ^{212}Pb-NNV003 were still alive at the end of the study, 21 weeks post cell injection. No significant difference between ^{212}Pb-NNV003 SAs was observed.

Haematological toxicity of ^{212}Pb-NNV003

In the R2G2 therapy study, two animals treated with 370 and 740 kBq ^{212}Pb-NNV003 died 9 days post injection of suspected acute radiotoxicity. 70% of the mice in the 370 kBq group survived for more than 28 weeks with no signs of toxicity, therefore we suspect that cause of death was poisoning during grooming. Further, two mice treated with 740 kBq were euthanised due to weight loss 165 and 191 days post cell inoculation. Necropsy observations showed no macroscopic tumours; however, small spleens and pale organs might indicate radiation damage. These results indicate that 740 kBq was a too high dose and confirm the HNSTD of 555 kBq in R2G2 mice. No toxicity was observed in the CB17 SCID mice treated with 280 kBq, thus this dose was determined as HNSTD for CB17 SCID mice.

At doses ranging from 185 to 555 kBq (R2G2) and 90 to 280 kBq (CB17 SCID), the haematological toxicity was modest. In R2G2 mice, but not in CB17 SCIDs, the platelet counts decreased one week after TAT injection, but only the 555 kBq treatment was significantly different from the NaCl treatment at week 1 and 3 (Fig 6A and 6B). The platelet counts also decreased in the untreated control group. We suggest this initial decrease in platelet counts to be due to the stress of being handled (three injections during three consecutive days) before blood sampling. Due to a shorter lifespan of controls, no reliable comparisons could be made after 3–4 weeks. The white blood cell- and red blood cell levels are presented in S5 Fig. Compared to controls and to baseline, no decrease in white blood cell- or red blood cell counts was observed in any of the studies.

Discussion

For the treatment of CLL and NHL patients, new therapies with different mechanisms of actions and targets are needed to further improve outcome. In the current study, a novel anti-CD37 TAT ^{212}Pb-NNV003 induced cytotoxicity in cell lines and was rapidly taken up in CD37 positive tumours. Furthermore, the TAT efficiently prolonged survival in CLL and NHL mouse models with up to 90% survival at the end of the study and low levels of haematological toxicity.

In mice injected with Daudi cells, 91% of the animals were still alive 28 weeks after receiving 90 kBq of ^{212}Pb-NNV003. In the MEC-2 model, doses of 370 kBq or more were needed to achieve similar effects. This corresponds well with the *in vitro* data showing that Daudi cells were more sensitive to ^{212}Pb-NNV003 compared to MEC-2 cells. Further, Daudi cells had higher and more homogeneous expression of CD37 than MEC-2 cells. MEC-2 cells present a more aggressive and invasive growth *in vivo*. Mice i.v. injected with MEC-2 cells were often euthanised due to weight loss after massive infiltration in several critical organs, while mice injected with Daudi cells were euthanised due to hind leg paralysis caused by localised infiltration of the bone marrow. Moreover, CB17 SCID mice have functional natural killer cells, whereas R2G2 do not, and the chimeric antibody NNV003 could induce some immunotherapeutic effect in this strain [8]. Accordingly, in a separate therapy study with Daudi-bearing CB17 SCID (S4 Fig) we observed that 5 μg NNV003 had a similar anti-tumour effect as 185 kBq ^{212}Pb-NNV003, while 100 μg NNV003 had no effect in the MEC-2 model. Therefore, the specific activity was increased to avoid any contribution of the antibody to the therapeutic effect, and the 0.75 μg NNV003 for 280 kBq used in the present study had no effect (Fig 5A)

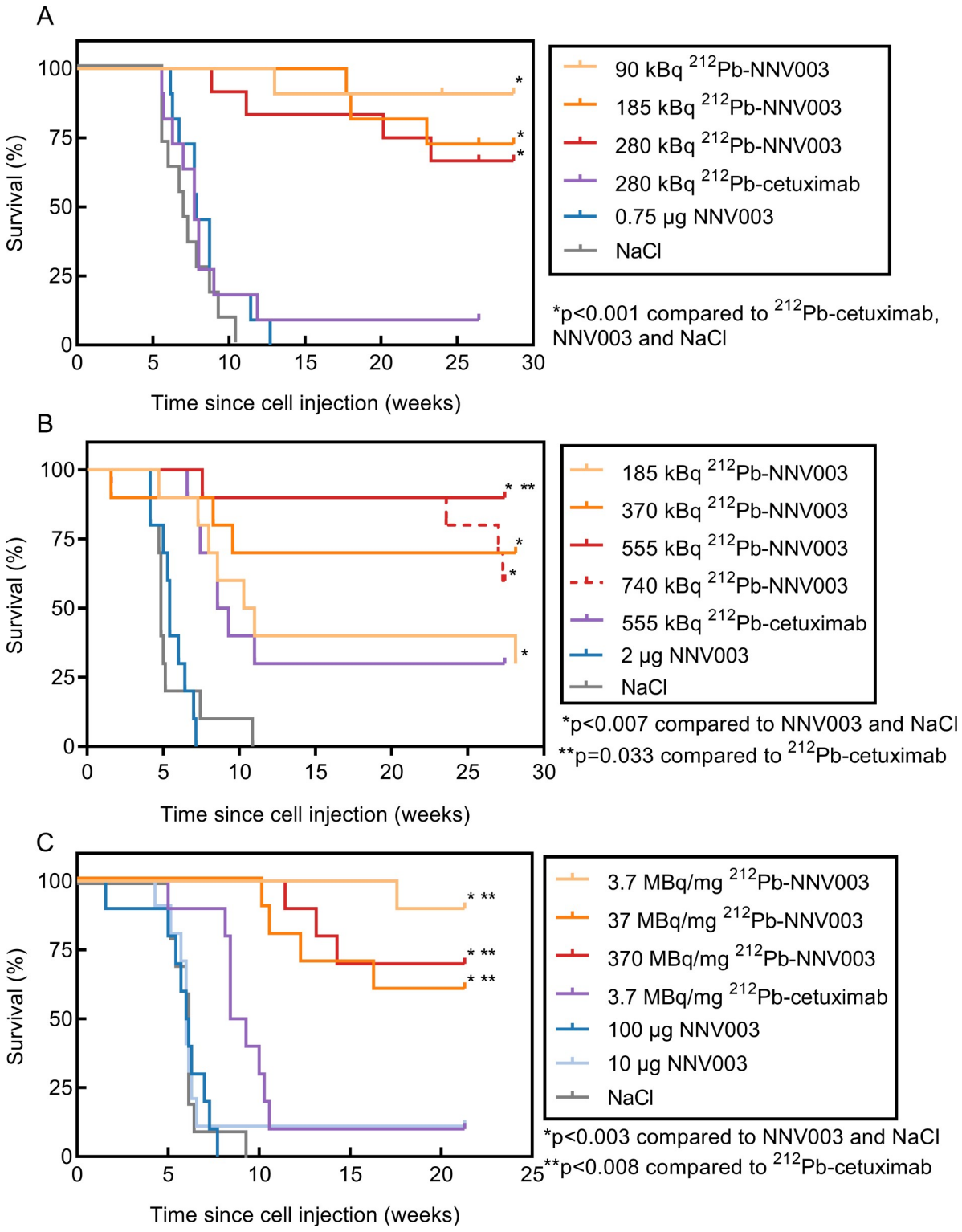

Fig 5. Anti-tumour effect of ^{212}Pb-NNV003. Survival of (A) CB17 SCID mice (n = 11 or 12) i.v. injected with Daudi cells and of (B) R2G2 mice (n = 10) i.v. injected with MEC-2 cells two days prior to treatment with ^{212}Pb-NNV003, ^{212}Pb-cetuximab, NNV003 or NaCl. (C) Survival of R2G2 mice (n = 10) i.v. injected with MEC-2 cells two days prior to treatment with 370 kBq ^{212}Pb-NNV003 with increasing SAs, ^{212}Pb-cetuximab, NNV003 or NaCl. Mice were censored at the end of the study.

https://doi.org/10.1371/journal.pone.0230526.g005

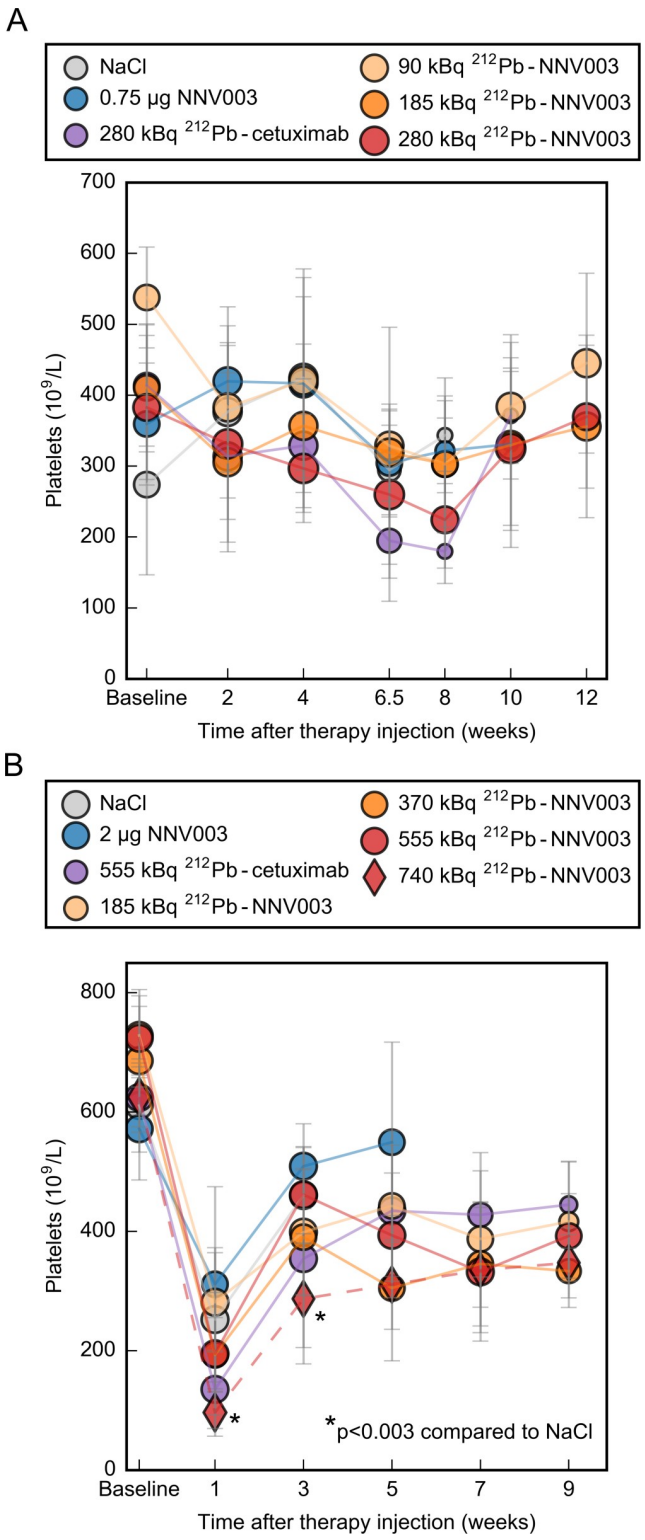

Fig 6. Haematological toxicity of ^{212}Pb-NNV003. Platelet counts from (A) CB17 SCID mice i.v. injected with Daudi cells two days before treatment and from (B) R2G2 mice i.v. injected with MEC-2 cells two days before treatment. Average with error bars = SD. Marker size represents the number of mice at each measurement, ranging from (A) 3–11 and (B) 4–10.

https://doi.org/10.1371/journal.pone.0230526.g006

In theory, α-particles are more suitable than β-particles for treatment of disseminated leukemic disease due to their short range and high level of cytotoxicity. Indeed, the survival rate after 90 kBq ^{212}Pb-NNV003 treatment, at less than half the HNSTD, was 91% in the Daudi model, whereas treatment with β-emitting ^{177}Lu-lilotomab satetraxetan at half the HNSTD, in the same animal model, led to 10% survival 28 weeks after therapy injection [9]. It is worth noting that lilotomab is the murine version of NNV003 and although they share the same epitope, it is not a direct comparison because of the difference in immunotherapeutic capacity [8]. Human IgG1 antibodies have been shown to bind stronger to mouse Fc receptors and induce more immunotherapeutic effect than mouse IgG1 [34]. However, the large difference between the treatments cannot be explained by this as the NNV003 dose was too low to have significant anti-tumour effect. This comparison supports the theory that α-particles are more advantageous against disseminated leukemic diseases.

The effect of different SAs was investigated to select a SA for a clinical trial. A clinically relevant SA is expected to be 3.7–7.4 MBq/mg, assuming that binding of 3–4 ^{212}Pb-NNV003 molecules is sufficient to eradicate a targeted cell [14]. In a phase 1 study of ^{212}Pb-TCMC-trastuzumab treatment, a single i.p. infusion of up to 27.4 MBq/m^2 was well tolerated [29], corresponding to approximately 50 MBq per patient. In our calculations we have assumed 5x10^6 B-lymphocytes/ml in a patient [36], 5 l blood and a CD37 expression of 1x10^5 antigens per cell [8]. An injection of 50 MBq ^{212}Pb-NNV003 with the SA of 3.7 MBq/mg (corresponding to 13.5 mg ^{212}Pb-NNV003), would lead to over 2x10^6 NNV003 molecules per cell and we can thus assume 100% occupancy of the antigen. The SA of 3.7 MBq/mg means that there is 51x10^{-6} ^{212}Pb nuclei per NNV003 antibody, which leads to 5.1 ^{212}Pb nuclei per cell. Consistently, we demonstrated that the anti-tumour effect of ^{212}Pb-NNV003 was independent of SAs in the range of 3.7 to 370 MBq/mg. The increase in unlabelled NNV003 in the 370 kBq treatment did not have a negative impact on the therapeutic effect of ^{212}Pb-NNV003.

The biodistribution of ^{212}Pb-NNV003 did not reveal any unexpected accumulation in normal organs and was similar to biodistributions of other ^{212}Pb labelled antibodies i.v. injected in mice. The uptake of ^{212}Pb-NNV003 in liver and kidneys is consistent with results from other studies [24, 37], while the accumulation in spleen of ^{212}Pb-NNV003 is lower than has been measured for another ^{212}Pb labelled antibody [24]. The accumulation of ^{212}Pb-NNV003 reached maximum after 24 h, resulting in an absorbed dose of 9.1 and 6.2 in the Daudi and MEC-2 tumours, respectively. A more rapid tumour targeting is expected in the i.v. models since the tumour cells are more accessible, and therefore a higher absorbed dose.

In the MEC-2 model, a modest anti-tumour effect was observed with the ^{212}Pb-labeled cetuximab treatment. Cetuximab does not bind to MEC-2 cells (S1 Fig). Thus, we speculate that the observed effect may be related to the co-localisation of tumour cells in blood-rich organs. MEC-2 cells infiltrated mostly organs with a high flow of radioactive blood in the hours after injection. Especially cells localised in the kidneys would be expected to receive a significant dose due to renal excretion of the TAT.

Female mice were used in these studies for practical reasons. Although they are less prone to kidney injuries than male mice, they are more sensitive to haematological toxicity of ionising radiation, and therefore represent the worst case scenario [38, 39]. As with other TATs for treatment of diseases with bone marrow involvement, haematological toxicity was expected to be dose limiting for ^{212}Pb-NNV003 [40–43]. A modest thrombocytopenia was observed in the MEC-2 model, but not in the Daudi model. No reduction in white blood cells or red blood cells was observed (S5 Fig). However, the white blood cell count in these immune deficient mice is generally lower at baseline than in other immunocompetent strains and are thus not well suited for monitoring haematological toxicity [44]. Furthermore, the total dose to femoral bone was low in both models, which might explain the modest haematological toxicity

observed. However, NNV003 does not bind to murine CD37 and hence only non-specific binding of ^{212}Pb-NNV003 will contribute to the absorbed radiation dose in the mice.

Around 35% of the gamma rays from ^{212}Pb decay to ^{212}Bi are internally converted, which can cause a ^{212}Bi-chelate complex to become unstable, and when using DOTA, 30% of the ^{212}Bi is released [45]. When using TCMC, 16% of ^{212}Bi is released (publication in preparation). If the released ^{212}Bi is circulating in the blood, it could have enough time to accumulate in the kidneys prior to decay, which could potentially be a source of non-targeted toxicity. Some indication of late radiation toxicity was observed in the 740 kBq group in the MEC-2 study, which might be due to this effect. However, the absorbed radiation doses to the kidneys at the HNSTDs (HNSTD based on haematological toxicity) were 2.5 Gy and 5.1 Gy (corresponding to 9.1 Gy/MBq, Fig 3), which is half of the dose that was found acceptable in a study with the alpha-emitter ^{211}At-MX35-F(ab')$_2$ [46].

The IRF of ^{212}Pb-NNV003 to CD37 was not measured before the studies were initiated and was probably around 50–60% based on post study measurements. The addition of ascorbic acid during labelling lead to an optimal IRF of around 80%, indicating that the problem was due to radiation induced oxidation and not due to the conjugation method. The IRF of ^{212}Pb-NNV003 did not seem to affect the efficacy of the TAT since the therapy studies showed long term efficacy even with a suboptimal binding, and a significantly higher anti-tumour effect than the non-binding control ^{212}Pb-cetuximab. We hypothesise that the increase in specific binding would lead to a better effect at lower doses of ^{212}Pb-NNV003 and studies have been initiated to confirm this.

We have shown that ^{212}Pb-NNV003 is effective and has a favourable safety profile in pre-clinical models of CD37 positive CLL and NHL. Future clinical testing is warranted.

Supporting information

S1 File. Supplementary material. Detailed description of animal models and supplementary method description.
(PDF)

S2 File. ARRIVE guidelines checklist.
(PDF)

S3 File. Raw data.
(XLSX)

S1 Table. Experimental animal models. Strain, age and average weight of experimental animals at the start of the studies.
(PDF)

S1 Fig. Binding of fluorescently labelled cetuximab. Flow cytometry histograms of cells (autofluorescence), cells blocked with unlabelled cetuximab and incubated with fluorescently labelled cetuximab (unspecific binding) and cells incubated with only fluorescently labelled cetuximab (total binding).
(TIF)

S2 Fig. Cytotoxic effect of ^{212}Pb-NNV003. Proliferation of Daudi and MEC-2 cells treated with ^{212}Pb-NNV003 or ^{212}Pb-cetuximab. Data represented as average of n = 8 replicates (n = 1–8 for ^{212}Pb-cetuximab) and error bars = SD.
(TIF)

S3 Fig. Biodistribution of ^{212}Pb-NNV003 with or without IgG2a predosing. %ID/g of ^{212}Pb-NNV003 in tissues of (A) CB17 SCID or (B) Balb/c mice with or without IgG2a predosing. n = 3 (no predosing Balb/c at 4 hours) or n = 5 (all other groups). Data presented as averages with error bars = SD, R = right, L = left, LPN = Lymph Node.
(TIF)

S4 Fig. Anti-tumour effect of ^{212}Pb-NNV003. Survival of CB17 SCID mice (n = 10 or 20) i.v. injected with Daudi cells two days prior to treatment with ^{212}Pb-NNV003 (37 MBq/mg), ^{212}Pb-cetuximab, NNV003 or NaCl. Mice were censored at the end of the study.
(TIF)

S5 Fig. Haematological toxicity of ^{212}Pb-NNV003. White blood cell counts (A and C) and red blood cell counts (B and D), measured in CB17 SCID mice i.v. injected with Daudi cells (A and B) and R2G2 mice i.v. injected with MEC-2 cells (C and D). There were 10–11 mice in each group at baseline. Marker size represents the number of mice at each measurement. Data is presented as average with error bars = SD.
(TIF)

Acknowledgments

The authors would like to thank Rapid (Maryland, USA) for the work on the dosimetry calculations.

Author Contributions

Conceptualization: Astri Fjelde Maaland, Amal Saidi, Julien Torgue, Helen Heyerdahl, Arne Kolstad, Jostein Dahle.

Data curation: Amal Saidi.

Formal analysis: Astri Fjelde Maaland, Amal Saidi.

Funding acquisition: Julien Torgue, Jostein Dahle.

Investigation: Amal Saidi.

Methodology: Astri Fjelde Maaland, Amal Saidi, Julien Torgue, Helen Heyerdahl, Tania A. Rozgaja Stallons, Arne Kolstad, Jostein Dahle.

Project administration: Amal Saidi.

Resources: Astri Fjelde Maaland, Amal Saidi, Julien Torgue, Helen Heyerdahl, Tania A. Rozgaja Stallons, Jostein Dahle.

Supervision: Amal Saidi, Julien Torgue, Helen Heyerdahl, Arne Kolstad, Jostein Dahle.

Visualization: Astri Fjelde Maaland, Amal Saidi.

Writing – original draft: Astri Fjelde Maaland.

Writing – review & editing: Astri Fjelde Maaland, Amal Saidi, Julien Torgue, Helen Heyerdahl, Arne Kolstad, Jostein Dahle.

References

1. Surveillance, Epidemiology, and End Results (SEER) Program Cancer Stat Facts—Chronic Lymphocytic Leukemia seer.cancer.gov2019 Available from: https://seer.cancer.gov/statfacts/html/clyl.html

2. Surveillance, Epidemiology, and End Results (SEER) Program Cancer Stat Facts—Non-Hodkin Lymphoma seer.cancer.gov2019 Available from: https://seer.cancer.gov/statfacts/html/nhl.html
3. Furman RR, Cheng S, Lu P, Setty M, Perez AR, Guo A, et al. Ibrutinib Resistance in Chronic Lymphocytic Leukemia. New England Journal of Medicine. 2014; 370(24):2352–4. https://doi.org/10.1056/NEJMc1402716 PMID: 24869597
4. Rezvani AR, Maloney DG. Rituximab resistance. Best practice & research Clinical haematology. 2011; 24(2):203–16.
5. Herling CD, Abedpour N, Weiss J, Schmitt A, Jachimowicz RD, Merkel O, et al. Clonal dynamics towards the development of venetoclax resistance in chronic lymphocytic leukemia. Nat Commun. 2018; 9(1):727. https://doi.org/10.1038/s41467-018-03170-7 PMID: 29463802
6. Tan D, Horning SJ, Hoppe RT, Levy R, Rosenberg SA, Sigal BM, et al. Improvements in observed and relative survival in follicular grade 1–2 lymphoma during 4 decades: the Stanford University experience. Blood. 2013; 122(6):981–7. https://doi.org/10.1182/blood-2013-03-491514 PMID: 23777769
7. Armitage JO, Gascoyne RD, Lunning MA, Cavalli F. Non-Hodgkin lymphoma. The Lancet. 2017; 390 (10091):298–310.
8. Maaland AF, Heyerdahl H, O'Shea A, Eiriksdottir B, Pascal V, Andersen JT, et al. Targeting B-cell malignancies with the beta-emitting anti-CD37 radioimmunoconjugate 177Lu-NNV003. European Journal of Nuclear Medicine and Molecular Imaging. 2019; 46(11):2311–21. https://doi.org/10.1007/s00259-019-04417-1 PMID: 31309259
9. Dahle J, Repetto-Llamazares AH, Mollatt CS, Melhus KB, Bruland OS, Kolstad A, et al. Evaluating antigen targeting and anti-tumor activity of a new anti-CD37 radioimmunoconjugate against non-Hodgkin's lymphoma. Anticancer Res. 2013; 33(1):85–95. PMID: 23267131
10. Beckwith KA, Frissora FW, Stefanovski MR, Towns WH, Cheney C, Mo X, et al. The CD37-targeted antibody–drug conjugate IMGN529 is highly active against human CLL and in a novel CD37 transgenic murine leukemia model. Leukemia. 2014; 28:1501. https://doi.org/10.1038/leu.2014.32 PMID: 24445867
11. Deckert J, Park PU, Chicklas S, Yi Y, Li M, Lai KC, et al. A novel anti-CD37 antibody-drug conjugate with multiple anti-tumor mechanisms for the treatment of B-cell malignancies. Blood. 2013; 122 (20):3500–10. https://doi.org/10.1182/blood-2013-05-505685 PMID: 24002446
12. Heider K-H, Kiefer K, Zenz T, Volden M, Stilgenbauer S, Ostermann E, et al. A novel Fc-engineered monoclonal antibody to CD37 with enhanced ADCC and high proapoptotic activity for treatment of B-cell malignancies. Blood. 2011; 118(15):4159–68. https://doi.org/10.1182/blood-2011-04-351932 PMID: 21795744
13. Kolstad A, Madsbu U, Beasley M, Bayne M, Illidge TM, O'Rourke N, et al. LYMRIT 37–01: A Phase I/II Study of 177lu-Lilotomab Satetraxetan (Betalutin®) Antibody-Radionuclide-Conjugate (ARC) for the Treatment of Relapsed Non-Hodgkin's Lymphoma (NHL)—Analysis with 6-Month Follow-up. Blood. 2018; 132(Suppl 1):2879-.
14. Gudkov SV, Shilyagina NY, Vodeneev VA, Zvyagin AV. Targeted Radionuclide Therapy of Human Tumors. International Journal of Molecular Sciences. 2016; 17(1).
15. Edem PE, Fonslet J, Kjaer A, Herth M, Severin G. In Vivo Radionuclide Generators for Diagnostics and Therapy. Bioinorganic Chemistry and Applications. 2016:6148357. https://doi.org/10.1155/2016/6148357 PMID: 28058040
16. Rotmensch J, Atcher RW, Schlenker R, Hines J, Grdina D, Block BS, et al. The effect of the α-emitting radionuclide lead-212 on human ovarian carcinoma: A potential new form of therapy. Gynecologic Oncology. 1989; 32(2):236–9. https://doi.org/10.1016/s0090-8258(89)80040-x PMID: 2910786
17. Horak E, Hartmann F, Garmestani K, Wu CC, Brechbiel M, Gansow OA, et al. Radioimmunotherapy targeting of HER2/neu oncoprotein on ovarian tumor using lead-212-DOTA-AE1. Journal of Nuclear Medicine. 1997; 38(12):1944–50. PMID: 9430475
18. Milenic DE, Garmestani K, Brady ED, Albert PS, Ma DS, Abdulla A, et al. alpha-particle radioimmunotherapy of disseminated peritoneal disease using a Pb-212-labeled radioimmunoconjugate targeting HER2. Cancer Biotherapy and Radiopharmaceuticals. 2005; 20(5):557–68. https://doi.org/10.1089/cbr.2005.20.557 PMID: 16248771
19. Boudousq V, Bobyk L, Busson M, Garambois V, Jarlier M, Charalambatou P, et al. Comparison between Internalizing Anti-HER2 mAbs and Non-Internalizing Anti-CEA mAbs in Alpha-Radioimmunotherapy of Small Volume Peritoneal Carcinomatosis Using Pb-212. Plos One. 2013; 8(7).
20. Milenic DE, Baidoo KE, Kim YS, Brechbiel MW. Evaluation of cetuximab as a candidate for targeted alpha-particle radiation therapy of HER1-positive disseminated intraperitoneal disease. mAbs. 2015; 7 (1):255–64. https://doi.org/10.4161/19420862.2014.985160 PMID: 25587678

21. Kasten BB, Arend RC, Katre AA, Kim H, Fan J, Ferrone S, et al. B7-H3-targeted 212Pb radioimmunotherapy of ovarian cancer in preclinical models. Nucl Med Biol. 2017; 47:23–30. https://doi.org/10.1016/j.nucmedbio.2017.01.003 PMID: 28104527

22. Milenic DE, Baidoo KE, Kim YS, Barkley R, Brechbiel MW. Targeted alpha-Particle Radiation Therapy of HER1-Positive Disseminated Intraperitoneal Disease: An Investigation of the Human Anti-EGFR Monoclonal Antibody, Panitumumab. Translational Oncology. 2017; 10(4):535–45. https://doi.org/10.1016/j.tranon.2017.04.004 PMID: 28577439

23. Kasten BB, Gangrade A, Kim H, Fan JD, Ferrone S, Ferrone CR, et al. Pb-212-labeled B7-H3-targeting antibody for pancreatic cancer therapy in mouse models. Nuclear Medicine and Biology. 2018; 58:67–73. https://doi.org/10.1016/j.nucmedbio.2017.12.004 PMID: 29413459

24. Kasten BB, Oliver PG, Kim H, Fan JD, Ferrone S, Zinn KR, et al. Pb-212-Labeled Antibody 225.28 Targeted to Chondroitin Sulfate Proteoglycan 4 for Triple-Negative Breast Cancer Therapy in Mouse Models. International Journal of Molecular Sciences. 2018; 19(4).

25. Miao YB, Hylarides M, Fisher DR, Shelton T, Moore H, Wester DW, et al. Melanoma therapy via peptide-targeted alpha-radiation. Clinical Cancer Research. 2005; 11(15):5616–21. https://doi.org/10.1158/1078-0432.CCR-05-0619 PMID: 16061880

26. Tan ZQ, Chen PP, Schneider N, Glover S, Cui LL, Torgue J, et al. Significant systemic therapeutic effects of high-LET immunoradiation by (212)pb-trastuzumab against prostatic tumors of androgen-independent human prostate cancer in mice. International Journal of Oncology. 2012; 40(6):1881–8. https://doi.org/10.3892/ijo.2012.1357 PMID: 22322558

27. Su FM, Beaumier P, Axworthy D, Atcher R, Fritzberg A. Pretargeted radioimmunotherapy in tumored mice using an in vivo Pb-212/Bi-212 generator. Nuclear Medicine and Biology. 2005; 32(7):741–7. https://doi.org/10.1016/j.nucmedbio.2005.06.009 PMID: 16243650

28. Shah MA, Zhang XL, Rossin R, Robillard MS, Fisher DR, Bueltmann T, et al. Metal-Free Cycloaddition Chemistry Driven Pretargeted Radioimmunotherapy Using alpha-Particle Radiation. Bioconjugate Chemistry. 2017; 28(12):3007–15. https://doi.org/10.1021/acs.bioconjchem.7b00612 PMID: 29129050

29. Meredith RF, Torgue JJ, Rozgaja TA, Banaga EP, Bunch PW, Alvarez RD, et al. Safety and Outcome Measures of First-in-Human Intraperitoneal alpha Radioimmunotherapy With 212Pb-TCMC-Trastuzumab. Am J Clin Oncol. 2018; 41(7):716–21. https://doi.org/10.1097/COC.0000000000000353 PMID: 27906723

30. Jeger S, Zimmermann K, Blanc A, Grunberg J, Honer M, Hunziker P, et al. Site-specific and stoichiometric modification of antibodies by bacterial transglutaminase. Angew Chem Int Ed Engl. 2010; 49(51):9995–7. https://doi.org/10.1002/anie.201004243 PMID: 21110357

31. Dennler P, Chiotellis A, Fischer E, Bregeon D, Belmant C, Gauthier L, et al. Transglutaminase-based chemo-enzymatic conjugation approach yields homogeneous antibody-drug conjugates. Bioconjug Chem. 2014; 25(3):569–78. https://doi.org/10.1021/bc400574z PMID: 24483299

32. Reddy N, Lin Ong G, Behr TM, Sharkey RM, Goldenberg DM, Mattes MJ. Rapid blood clearance of mouse IgG2a and human IgG1 in many nude and nu/+ mouse strains is due to low IgG2a serum concentrations. Cancer Immunology, Immunotherapy. 1998; 46(1):25–33. https://doi.org/10.1007/s002620050456 PMID: 9520289

33. Dekkers G, Bentlage AEH, Stegmann TC, Howie HL, Lissenberg-Thunnissen S, Zimring J, et al. Affinity of human IgG subclasses to mouse Fc gamma receptors. mAbs. 2017; 9(5):767–73. https://doi.org/10.1080/19420862.2017.1323159 PMID: 28463043

34. Overdijk MB, Verploegen S, Ortiz Buijsse A, Vink T, Leusen JH, Bleeker WK, et al. Crosstalk between human IgG isotypes and murine effector cells. J Immunol. 2012; 189(7):3430–8. https://doi.org/10.4049/jimmunol.1200356 PMID: 22956577

35. Fulop GM, Phillips RA. The scid mutation in mice causes a general defect in DNA repair. Nature. 1990; 347(6292):479–82. https://doi.org/10.1038/347479a0 PMID: 2215662

36. Eichhorst B, Robak T, Montserrat E, Ghia P, Hillmen P, Hallek M, et al. Chronic lymphocytic leukaemia: ESMO Clinical Practice Guidelines for diagnosis, treatment and follow-up. Ann Oncol. 2015; 26 Suppl 5:v78–84.

37. Schneider NR, Lobaugh M, Tan Z, Sandwall P, Chen P, Glover SE, et al. Biodistribution of Pb-212 conjugated trastuzumab in mice. Journal of Radioanalytical and Nuclear Chemistry. 2013; 296(1):75–81.

38. Billings. Effect of Gender on the Radiation Sensitivity of Murine Blood Cells. Gravit Space Res. 2015.

39. Kang KP, Lee JE, Lee AS, Jung YJ, Kim D, Lee S, et al. Effect of gender differences on the regulation of renal ischemia-reperfusion-induced inflammation in mice. Molecular medicine reports. 2014; 9(6):2061–8. https://doi.org/10.3892/mmr.2014.2089 PMID: 24682292

40. Jurcic JG, Larson SM, Sgouros G, McDevitt MR, Finn RD, Divgi CR, et al. Targeted α particle immunotherapy for myeloid leukemia. Blood. 2002; 100(4):1233–9. PMID: 12149203

41. Rosenblat TL, McDevitt MR, Mulford DA, Pandit-Taskar N, Divgi CR, Panageas KS, et al. Sequential cytarabine and alpha-particle immunotherapy with bismuth-213-lintuzumab (HuM195) for acute myeloid leukemia. Clin Cancer Res. 2010; 16(21):5303–11. https://doi.org/10.1158/1078-0432.CCR-10-0382 PMID: 20858843

42. Jurcic JG, Levy MY, Park JH, Ravandi F, Perl AE, Pagel JM, et al. Phase I Trial of Targeted Alpha-Particle Therapy with Actinium-225 (Ac-225)-Lintuzumab and Low-Dose Cytarabine (LDAC) in Patients Age 60 or Older with Untreated Acute Myeloid Leukemia (AML). Blood. 2016; 128(22).

43. Atallah EL, Orozco JJ, Craig M, Levy MY, Finn LE, Khan SS, et al. A Phase 2 Study of Actinium-225 (Ac-225)-Lintuzumab in Older Patients with Untreated Acute Myeloid Leukemia (AML)—Interim Analysis of 1.5 mu ci/Kg/Dose. Blood. 2018;132. https://doi.org/10.1182/blood-2018-01-769018

44. Nemzek JA, Bolgos GL, Williams BA, Remick DG. Differences in normal values for murine white blood cell counts and other hematological parameters based on sampling site. Inflamm Res. 2001; 50 (10):523–7. https://doi.org/10.1007/PL00000229 PMID: 11713907

45. Mirzadeh S, Kumar K, Gansow OA. The Chemical Fate of 212Bi-DOTA Formed by β- Decay of 212Pb (DOTA)2-. Radiochimica Acta. 1993; 60(1):1–10.

46. Back T, Haraldsson B, Hultborn R, Jensen H, Johansson ME, Lindegren S, et al. Glomerular filtration rate after alpha-radioimmunotherapy with 211At-MX35-F(ab')2: a long-term study of renal function in nude mice. Cancer Biother Radiopharm. 2009; 24(6):649–58. https://doi.org/10.1089/cbr.2009.0628 PMID: 20025544

Collaboration with Toulouse University Hospitals

^{212}Pb α-Radioimmunotherapy Targeting CD38 in Multiple Myeloma: A Preclinical Study

Isabelle Quelven[1,2], Jacques Monteil[1,2], Magali Sage[2], Amal Saidi[3], Jérémy Mounier[2], Audrey Bayout[1], Julie Garrier[2], Michel Cogne*[2], and Stéphanie Durand-Panteix*[2]

[1]Nuclear Medicine Department, Limoges University Hospital, Limoges, France; [2]CNRS-UMR7276, INSERM U1262, Contrôle de la Réponse Immune B et Lymphoprolifération, Limoges University, Limoges, France; and [3]Orano Med SAS, Paris, France

Multiple myeloma (MM) is a plasma cell cancer and represents the second most frequent hematologic malignancy. Despite new treatments and protocols, including high-dose chemotherapy associated with autologous stem cell transplantation, the prognosis of MM patients is still poor. α-radioimmunotherapy (α-RIT) represents an attractive treatment strategy because of the high-linear-energy transfer and short pathlength of α-radiation in tissues, resulting in high tumor cell killing and low toxicity to surrounding tissues. In this study, we investigated the potential of α-RIT with ^{212}Pb-daratumumab (anti-hCD38), in both in vitro and in vivo models, as well as an antimouse CD38 antibody using in vivo models. **Methods:** Inhibition of cell proliferation after incubation of the RPMI8226 cell line with an increasing activity (0.185–3.7 kBq/mL) of ^{212}Pb-isotypic control or ^{212}Pb-daratumumab was evaluated. Biodistribution was performed in vivo by SPECT/CT imaging and after death. Dose-range–finding and acute toxicity studies were conducted. Because daratumumab does not bind the murine CD38, biodistribution and dose-range finding were also determined using an antimurine CD38 antibody. To evaluate the in vivo efficacy of ^{212}Pb-daratumumab, mice were engrafted subcutaneously with 5×10^6 RPMI8226 cells. Mice were treated 13 d after engraftment with an intravenous injection of ^{212}Pb-daratumumab or control solution. Therapeutic efficacy was monitored by tumor volume measurements and overall survival. **Results:** Significant inhibition of proliferation of the human myeloma RPMI8226 cell line was observed after 3 d of incubation with ^{212}Pb-daratumumab, compared with ^{212}Pb-isotypic control or cold antibodies. Biodistribution studies showed a specific tumoral accumulation of daratumumab. No toxicity was observed with ^{212}Pb-daratumumab up to 370 kBq because of lack of cross-reactivity. Nevertheless, acute toxicity experiments with ^{212}Pb-anti-mCD38 established a toxic activity of 277.5 kBq. To remain within realistically safe treatment activities for efficacy studies, mice were treated with 185 kBq or 277.5 kBq of ^{212}Pb-daratumumab. Marked tumor growth inhibition compared with controls was observed, with a median survival of 55 d for 277.5 kBq of ^{212}Pb-daratumumab instead of 11 d for phosphate-buffered saline. **Conclusion:** These results showed ^{212}Pb-daratumumab to have efficacy in xenografted mice, with significant tumor regression and increased survival. This study highlights the potency of α-RIT in MM treatment.

Key Words: ^{212}Pbα-radioimmunotherapy; multiple myeloma; CD38

J Nucl Med 2020; 61:1058–1065
DOI: 10.2967/jnumed.119.239491

Multiple myeloma (MM) features monoclonal proliferation of plasma cells in bone marrow. Over the last decade, many advances have been made in MM therapy, and the median life expectancy of patients has almost doubled. This improvement was mostly due to the development of proteasome inhibitors, immunomodulatory drugs, histone deacetylase blockers, and, more recently, monoclonal antibodies (mAbs) (daratumumab and elotuzumab) (*1*). However, the prognosis of myeloma patients remains poor, since remission obtained with such treatments is often followed by relapse. Innovative therapies with a distinct mechanism of action are therefore needed.

Targeted immunotherapy using mAbs has showed efficacy; nevertheless, strategies to enhance mAb efficiency are necessary and were developed in the form of antibody–drug conjugates, immunotoxins, or radiolabeled antibodies. The efficacy of radioimmunotherapy (RIT) in the treatment of non-Hodgkin lymphoma is well established, with there being 2 marketed anti-CD20 mAbs coupled with β-emitters: ^{90}Y-ibritumomab tiuxetan (Zevalin; Acrotech Biopharma, LLC) and ^{131}I-tositumomab (Bexxar; GlaxoSmithKline) (*2*). Although ^{90}Y-ibritumomab tiuxetan is highly efficient against tumor cells, it carries severe side effects compared with rituximab, notably bone marrow toxicity. Since α-particles have a short pathlength of 50–80 μm (compared with a few millimeters for β-particles), RIT with α-emitting radionuclides is highly attractive and expected to reduce unwanted radiation exposure on normal tissues. The short pathlength of α-particles also explains why α-RIT, by specifically targeting the close environment of each malignant cell, is better suited for micrometastatic and disseminated tumor treatment (*3*). α-particles produce clustered DNA double-strand breaks and highly reactive hydroxyl radicals when hitting biologic tissues. Their short path range leads to a high-linear-energy transfer of approximately 50–230 keV/μm, compared with 0.1–1.0 keV/μm for β-emitters, making α-emitters 100-fold more cytotoxic. Only a few α-emitters are considered suitable for therapeutic use in cancer patients (*4*). ^{212}Pb represents a good candidate. This radioelement is available at high purity through a ^{224}Ra/^{212}Pb generator. After administration, ^{212}Pb (β-emitter)

Received Nov. 10, 2019; revision accepted Nov. 18, 2019.
For correspondence or reprints contact: Michel Cogne, CNRS UMR 7276 – INSERM U1262, CRIBL, Limoges University, Rue Bernard Descottes, CBRS, CNRS/INSERM, Limoges, 87025, France
E-mail: michel.cogne@unilim.fr
*Contributed equally to this work.
Published online Dec. 20, 2019.

generates ^{212}Bi (α-emitter); thus, ^{212}Pb, which has a half-life (10.6 h) relatively convenient for mAb pharmacokinetics, serves as an in vivo α-emitter generator (*5*). A macrocyclic bifunctional ligand, TCMC (1.4.7.10-tetra-(2-carbamoyl methyl)-cyclododecane), was designed and synthesized to obtain a greater stability in vivo for the chelation of lead isotopes (*6*). mAb can therefore be easily functionalized with TCMC and then radiolabeled with ^{212}Pb. ^{212}Pb was first used in a human trial of ^{212}Pb-TCMC-trastuzumab in patients with HER2–expressing malignancies (*7,8*).

CD38, a 45-kDa stable transmembrane glycoprotein receptor, is expressed at a high epitope density on 95%–100% of malignant plasma cells (*9,10*). The CD38 antigen is expressed on activated T cells, monocytes, and NK (natural killer) cells but at much lower levels than found on plasma cells, making it a targeting candidate for RIT using anti-CD38 antibodies. Few RIT studies have evaluated this target potency, and none have evaluated ^{212}Pb-anti-CD38 RIT in myeloma. Daratumumab is an antihuman CD38 developed by Janssen and currently used in the clinic (*11*). We have developed a targeted α-therapy in which the daratumumab antibody is coupled to the α-particle–emitting radioisotope ^{212}Pb. The goal of this study was to investigate the potential of ^{212}Pb-daratumumab in the treatment of plasma cell malignancies. Biodistribution and toxicity studies were performed on tumor-free and RPMI 8226 myeloma tumor–bearing mice. Considering that ^{212}Pb-daratumumab does not cross-react with the murine CD38, biodistribution and toxicity studies were also performed with an antimurine CD38 mAb. The therapeutic efficacy of this treatment was assessed in vitro and in vivo on a subcutaneous xenograft model.

MATERIALS AND METHODS

Cell Lines and Mice

The human myeloma RPMI8226 cell line (ATCC) was maintained in supplemented RPMI 1640 medium. C57BL/6 mice (female, 7–10 wk old) were purchased from Janvier Labs. Rag2$^{-/-}\gamma C^{-/-}$ mice were kindly provided by Dr. James Di Santo (Institut Pasteur).

Xenograft Models

Rag2$^{-/-}\gamma C^{-/-}$ mice 8–12 wk old received a subcutaneous graft of 5×10^6 RPMI8226 cells in the leg flank (in 100 μL of phosphate-buffered saline [PBS] and Matrigel [Corning] 50/50, v/v). The mice were monitored daily for signs of pain or discomfort. Tumor volume was measured with a caliper 3 times a week. Studies were conducted 13 d after engraftment (tumors between 150 and 400 mm^3), except for SPECT/CT imaging (20 d/500–800 mm^3). All in vivo experiments were performed in accordance with animal ethical rules, and all protocols were authorized by the French Ministry of Research according to European Union regulations (APAFIS 15900-201807061621591, version 2).

mAb Conjugation and Radiolabeling

mAbs were obtained from Janssen: IgG antihuman CD38 (anti-hCD38) (daratumumab), IgG isotypic control, and IgG antimurine CD38 (anti-mCD38, which is not a surrogate of daratumumab as it lacks the in vitro and in vivo functional activity of the anti-hCD38 antibody). Antibodies were conjugated by Macrocyclics with the bifunctional chelating agent TCMC using a proprietary site-specific technique, with approximately 1.3–2 TCMC/mAb.

^{212}Pb was produced from ^{224}Ra generators provided by Orano Med SAS. Chelation was performed by incubating 1 mg of mAb-TCMC per 37 MBq of ^{212}Pb for 15 min at 37°C in 150 mM ammonium acetate, pH 4.5. The labeling yield, assayed by instant thin-layer chromatography, was more than 94%, and specific activity was approximately 37 MBq/mg for the mAbs at the experiment time. The immunoreactivity of ^{212}Pb-daratumumab against hCD38 was assessed in vitro, by direct binding assays (*12*) on RPMI8226 cells, and a dissociation constant of 2.69 ± 1.28 nM was obtained. This value is consistent with known daratumumab affinity (4.36 nM) (*13*). Furthermore, an immunoreactive fraction of more than 92% was obtained. For SPECT/CT imaging, mAbs were radiolabeled with ^{203}Pb. ^{203}Pb in 0.5 M HCl was provided by Lantheus Medical Imaging. After the pH of the ^{203}Pb solution had been adjusted to 4.5 with 1.5 M ammonium acetate, mAbs were incubated for 15 min with ^{203}Pb at 37°C. The labeling yield was more than 98%, and specific activity was approximately 37 MBq/mg.

Cell Proliferation Analyses

RPMI8226 cells were cultured at 37°C in 96-well plates (25,000 cells in 100 μL/well). Proliferation was assessed in triplicate on days 1–4, under various concentrations of ^{212}Pb-mAb (0.185–3.7 kBq/mL) or cold mAb (5–100 ng/mL) using Cell Titer Glo (incubation, 2 h; optical density, 490 nm) (Promega).

Biodistribution Experiments and SPECT/CT Imaging

Biodistribution experiments were performed on tumor-free or tumor-bearing C57BL/6 or Rag2$^{-/-}\gamma C^{-/-}$ mice. ^{212}Pb-anti-mCD38, ^{212}Pb-daratumumab, or ^{212}Pb-isotypic control (1.85 MBq) was injected intravenously. At each time point (2, 6, 12, 18, 24, and 48 h after injection), 2–5 animals per group were euthanized under isoflurane inhalational anesthesia by cervical dislocation. Selected tissues were excised and weighed, and their radioactivity levels were measured with a calibrated γ-counter (Perkin Elmer) (190–290 keV). The uptake of radioactivity in these organs was expressed as percentage injected dose (%ID)/g after correcting for radioactive decay at each time point.

For SPECT/CT imaging, the animals were injected with ^{203}Pb-mAbs (18.5 MBq) and imaged under isoflurane inhalational anesthesia (1.8%, 50% air/50% oxygen, 1.4 L/min) at 2, 6, 24, 48, and 96 h after injection with a small-animal SPECT/CT scanner (U-SPECT4/CT; MILabs). Image acquisition lasted 30 min for earlier time-points to 90 min for later time-points. Energy windows were set over the 279-keV peak (±20%), and a general-purpose rat-and-mouse collimator was used (75 holes of 1.5-mm diameter, iterative reconstruction ordered-subsets expectation maximization, and no filter [16 subsets, 6 iterations, and a voxel size of 0.8 mm]). The SPECT resolution with ^{203}Pb is estimated to be less than 1 mm. Images were analyzed with PMOD Software (PMOD Technologies).

Toxicity Studies

Groups of 5–8 tumor-free mice (C57BL/6 or Rag2$^{-/-}\gamma C^{-/-}$) received ^{212}Pb-daratumumab, ^{212}Pb-anti-mCD38 (185–370 kBq), or PBS by intravenous injection. Mice were monitored and weighed daily. At the experimental time point, a complete blood count was performed on an automated hematology analyzer (Cell Dyn; Abbott). Biochemical parameters (aspartate transaminase, alanine transaminase, urea, and creatinine) were measured in blood plasma on an automated biochemistry analyzer (Konelab; Thermo). The percentage of B220-positive cells in blood, bone marrow, and spleen was determined by flow cytometry (AccuriC6; BD). We took advantage of the coexpression of B220 and CD38 (*14*) to monitor variations in B-lineage using a B220 labeling.

RIT Experiments

Mice were randomly assigned to experimental groups and received a single intravenous injection of ^{212}Pb-daratumumab (185 kBq or

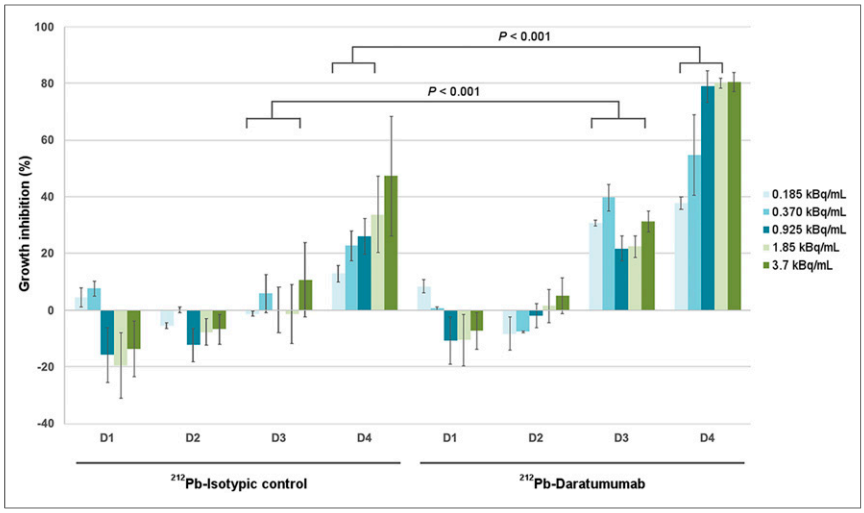

FIGURE 1. Percentage of growth inhibition for increasing activity of ^{212}Pb-mAbs. RPMI8226 cell growth inhibition percentage was calculated, from day 1 to day 4, using untreated cells as controls on same day. Growth inhibition is calculated as $[(1 - OD_{treatment}/OD_{control}) \times 100] \pm$ SEM. OD = optical density.

277.5 kBq), ^{212}Pb-isotypic control (277.5 kBq), daratumumab (10 μg), daratumumab (16 mg/kg), or PBS. The mice were monitored daily for general appearance. Twice a week, tumor volume was measured and the mice were weighed. They were euthanized when tumors reached a volume of 1 cm^3, when tumor ulceration occurred, or when the tumor was causing obvious discomfort.

RESULTS

^{212}Pb Irradiation–Induced Inhibition of Proliferation of MM Cells

The effect on cell proliferation of increasing activity (0.185–3.7 kBq/mL) of ^{212}Pb-daratumumab or ^{212}Pb-isotypic control was assessed during 4 d (Fig. 1). Growth inhibition was observed with ^{212}Pb-daratumumab from day 3, with a dose-dependent inhibition at day 4 (37.7% ± 2.3% at 0.185 kBq/mL to 80.6% ± 3.4% at 3.7 kBq/mL). This inhibition was significantly higher than ^{212}Pb-isotypic control inhibition at all activities tested except for 3.7 kBq/mL. The same experiment with increasing concentrations of the 2 cold mAbs showed no significant effect on growth inhibition (Supplemental Fig. 1; supplemental materials are available at http://jnm.snmjournals.org).

Biodistribution Experiments and SPECT/CT Imaging

Biodistribution of daratumumab was studied in Rag2$^{-/-}\gamma C^{-/-}$ tumor-bearing mice to monitor daratumumab-specific accumulation in the human tumor xenograft and was compared with an

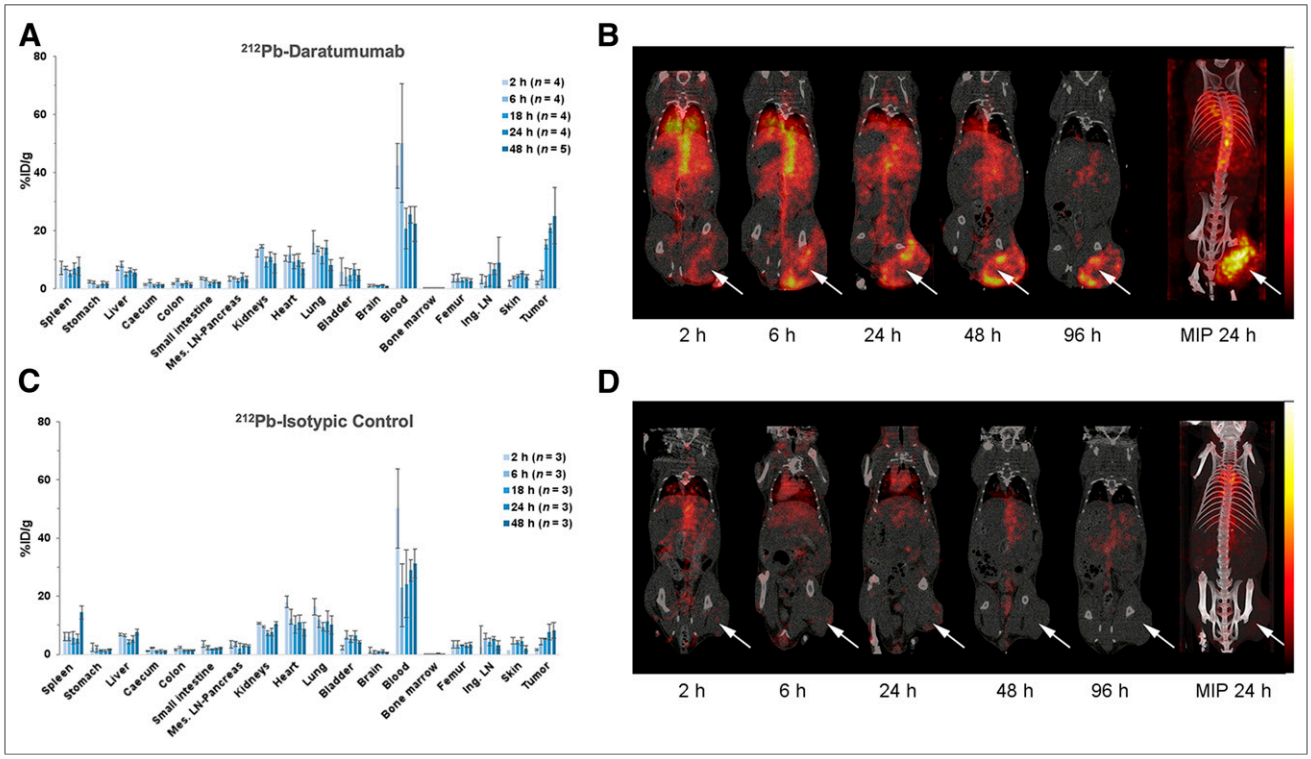

FIGURE 2. Biodistribution of radiolabeled daratumumab (A and B) and isotypic control (C and D) in mice bearing RPMI8226 xenograft. (A and C) For postmortem biodistribution studies, mice were injected with 185 kBq of ^{212}Pb-daratumumab (A) or ^{212}Pb-isotypic control (C). Radioactivity in tumor, organs, and blood was expressed as %ID/g. Radioactivity in tumor significantly differs between the 2 mAbs ($P < 0.001$). (B and D) For in vivo imaging studies, 7.4 MBq of ^{203}Pb-daratumumab (B) or ^{212}Pb-isotypic control (D) were injected. Mice were imaged by small-animal SPECT/CT 2, 6, 24, 48, and 96 h after injection. Tumors are indicated by arrows. Ing. LN = inguinal lymph node; Mes. LN = mesenteric lymph node; MIP = maximum-intensity projection.

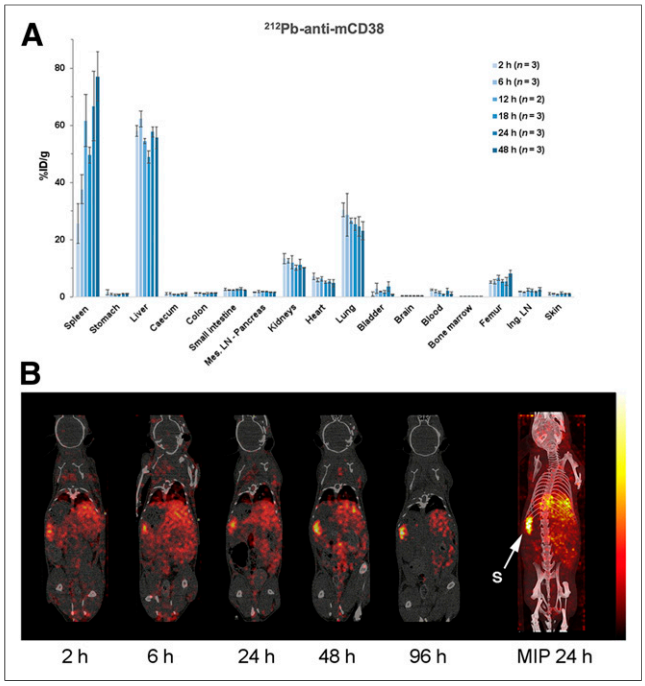

FIGURE 3. Biodistribution of radiolabeled anti-mCD38 in C57BL/6 healthy mice. (A) For postmortem biodistribution studies, mice were injected with 185 kBq of ^{212}Pb-anti-mCD38. Radioactivity was expressed as %ID/g of tissue. (B) For in vivo studies, mice were imaged by small-animal SPECT/CT 2, 6, 24, 48, and 96 h after injection of ^{203}Pb-anti-mCD38 (7.4 MBq). Ing. LN = inguinal lymph node; Mes. LN = mesenteric lymph node; MIP = maximum-intensity projection; S = spleen.

isotypic control (Fig. 2). After ^{212}Pb-daratumumab injection, radioactivity in the tumors increased over time: peak radioactivity was reached after 24 h (20.8 ± 1.4 %ID/g), and this high level was maintained at 48 h after injection. From 18 h, accumulation of ^{212}Pb-daratumumab in the tumor was significantly higher than that of ^{212}Pb-isotypic control (7.75 ± 2.6 %ID/g at 24 h). In vivo, imaging data confirmed specific tumoral accumulation of daratumumab, with a peripheral tumoral uptake for larger tumors (Figs. 2C and 2D). The accumulation of ^{212}Pb-daratumumab and ^{212}Pb-isotypic control in all nontumor tissues did not significantly differ.

Because daratumumab does not bind mCD38, a biodistribution study using an anti-mCD38 antibody was performed on tumor-free mice to estimate antibody accumulation in healthy organs and anticipate potential toxicity issues. Biodistribution studies on C57BL/6 mice showed high accumulation of radioactivity in 3 organs as soon as 2 h after injection: liver (58.1 ± 1.9 %ID/g), spleen (25.7 ± 6.9 %ID/g), and lung (30.5 ± 2.4 %ID/g) (Fig. 3). Uptake was then relatively constant over time in these organs, except for the spleen, in which the radioactivity increased with time (66.8 %ID/g at 24 h). Significant radioactivity was also present in the femur (6%–8%), but radioactivity remained low in the blood (<2% after 6 h). The biodistribution of anti-mCD38 was also examined in Rag2$^{-/-}\gamma C^{-/-}$ (Supplemental Fig. 2), and a similar pattern was observed, except for a higher uptake in the spleen (134.6 %ID/g at 24 h) due to the splenic hypotrophy of Rag-deficient mice, as observed on SPECT/CT images.

Compared with ^{212}Pb-anti-mCD38, ^{212}Pb-daratumumab accumulation in spleen, liver, lung, bone marrow, and femur was lower.

Dose-Range Finding and Acute Toxicity

Anti-hCD38/Daratumumab. Acute toxicity (7 and 21 d) was studied after injection of 185, 277.5, or 370 kBq of ^{212}Pb-daratumumab in Rag2$^{-/-}\gamma C^{-/-}$ healthy mice. For these 3 activity levels, no effect was observed on survival (Table 1), body weight, blood cell count, or biochemical doses (data not shown), consistent with daratumumab's lack of binding to mCD38. For that reason, toxicity was thus also studied with anti-mCD38.

Anti-mCD38. The acute toxicity of 185 and 370 kBq of ^{212}Pb-anti-mCD38 was studied in C57BL/6 and in Rag2$^{-/-}\gamma C^{-/-}$ healthy mice. Animal behavior and body weight were monitored during 21 d. For both strains, a significant body weight loss ($P < 0.01$) was observed after 185 kBq of ^{212}Pb-anti-mCD38 compared with PBS (Fig. 4; Supplemental Fig. 3). This loss was dose-dependent and significantly increased with 370 kBq of ^{212}Pb-anti-mCD38 ($P < 0.0001$). Survival was not affected after injection of 185 kBq of ^{212}Pb-anti-mCD38, whereas 370 kBq of ^{212}Pb-anti-mCD38 induced 75% lethality for C57BL/6 and 40% for Rag2$^{-/-}\gamma C^{-/-}$ mice at the 21-d time point (Table 1).

TABLE 1
Mice Surviving After Acute Toxicity Study

Mouse	Treatment	Activity (kBq)	Surviving mice at endpoint (*n*)	
			7 d	21 d
Rag2$^{-/-}\gamma C^{-/-}$	PBS		5/5	5/5
	^{212}Pb-daratumumab	185	5/5	5/5
		277.5	5/5	5/5
		370	5/5	5/5
	^{212}Pb-anti-mCD38	185	5/5	5/5
		370	4/5*	3/5*
C57BL/6	PBS		5/5	5/5
	^{212}Pb-anti-mCD38	185	6/6	6/6
		370	8/8	2/8*

*Some mice did not survive to endpoint.

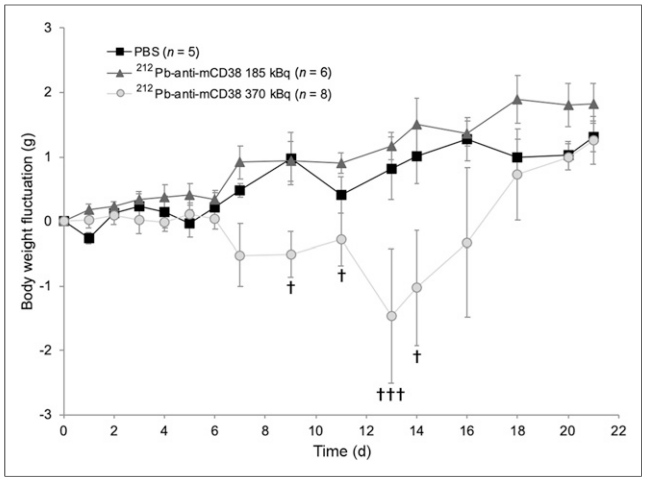

FIGURE 4. Body weight variations of C57BL/6 mice after acute toxicity study. Mice were injected intravenously with PBS or 185 or 370 kBq of ^{212}Pb-anti-mCD38. Variations in body weight relative to day 0 are represented. †Mice euthanized.

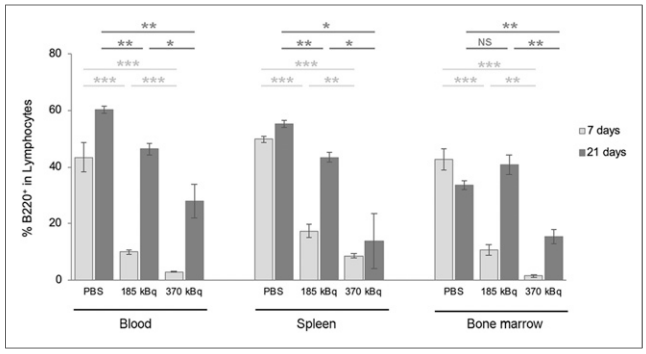

FIGURE 6. Effect of acute toxicity on B220 cells of lymphoid organs. C57BL/6 mice were injected intravenously with PBS or 185 or 370 kBq of ^{212}Pb-anti-mCD38. At endpoint, 7 or 21 d, blood (left), spleen (middle), and bone marrow (right) were excised and analyzed. NS = $P >$ 0.05. *$P < 0.05$. **$P < 0.01$. ***$P < 0.001$.

In C57BL/6 mice, we investigated kidney and liver toxicity using biochemical quantification of plasma creatinine, urea (kidney toxicity), aspartate transaminase, and alanine transaminase (liver toxicity). No significant changes in these amounts were observed (Supplemental Fig. 4). Complete blood cell counts revealed hematologic toxicity, with a drop in both leukocyte and platelet counts, whereas red blood cell count was not affected by ^{212}Pb-anti-mCD38 injection (Fig. 5). At 7 and 10 d after injection, the leukocyte counts were reduced to the lower limit of the reference ranges for 185 kBq and below the reference ranges for 370 kBq (Fig. 5A). The leukocyte decrease was reversible for both activity levels, and values were back to normal 21 d after injection. In the same way, platelet counts were reduced at as early as 7 d, but no recovery was observed at day 21 (Fig. 5C). Fluorescence-activated cell sorting analyses of the B220 population in blood, spleen, and bone marrow (Fig. 6) confirmed these results and radiation-induced spleen and bone marrow damage.

Acute toxicity manifested at 370 kBq of ^{212}Pb-anti-mCD38, and therapeutic activity should thus remain below this dose.

Efficacy of ^{212}Pb-Daratumumab Treatment

Efficacy studies were conducted on Rag2$^{-/-}\gamma C^{-/-}$ bearing subcutaneous xenografts of RPMI8226 MM cells. Survival curves and tumoral growth after treatment are presented in Figure 7. In the control group (PBS), a median survival of 11 d was observed (Fig. 7A). All treatments except daratumumab at 10 μg (equivalent amount used for the radiolabeled antibody) induced a significant median survival time increase ($P < 0.001$): 32, 39.5, 47, and 55.5 d for daratumumab at 16 mg/kg (dose used in clinical practice), ^{212}Pb-isotypic control at 277.5 kBq, and ^{212}Pb-daratumumab at 185 kBq and 277.5 kBq, respectively. Nevertheless, the survival increase induced by ^{212}Pb-daratumumab at 277.5 kBq was significantly higher than that with cold daratumumab ($P < 0.001$). ^{212}Pb-daratumumab at 277.5 kBq induced a tumoral regression from day 4 to day 25 after treatment, but a resumption of tumoral growth was then observed except for 1 mouse (Fig. 7B).

DISCUSSION

Recent advances in MM therapies, such as immunomodulatory drugs and proteasome inhibitors, have significantly prolonged the survival of MM patients over the last decade. However, the prognosis for patients with relapsed MM remains poor. RIT is a therapeutic modality that is not cross-resistant with chemotherapy or other therapeutic agents. This strategy has already shown its value in hematologic cancers, but there are few studies on RIT in MM.

Chérel et al. have studied RIT efficiency in MM with ^{213}Bi-anti-CD138 and showed significant efficacy in murine myeloma models (*15*). In our study, we targeted CD38 because its expression is high and uniform on malignant plasma cells but relatively low on normal lymphoid and myeloid cells and on nonhematopoietic tissues (*16*). Recent

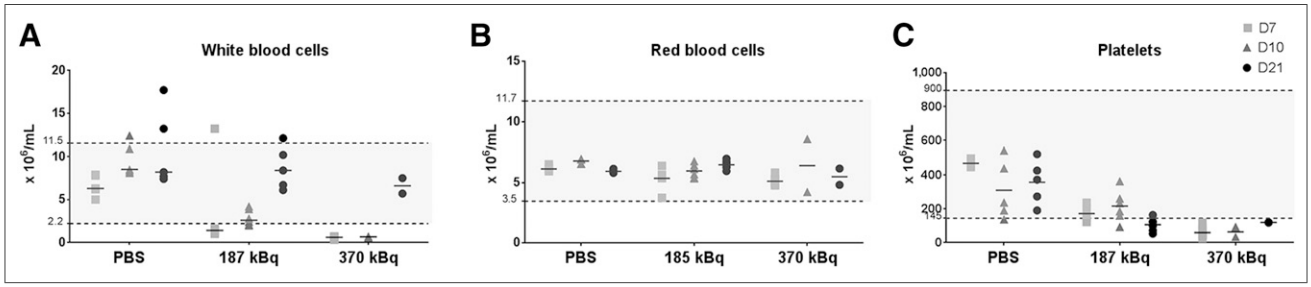

FIGURE 5. Effect of acute toxicity on blood cell counts. C57BL/6 mice were injected intravenously with PBS or 185 or 370 kBq of ^{212}Pb-anti-mCD38. Mice followed over 7 d were euthanized, and blood samples were analyzed. For mice followed over 21 d, blood samples were analyzed on days 10 and 21. Results for white blood cells (A), red blood cells (B), and platelets (C) are represented.

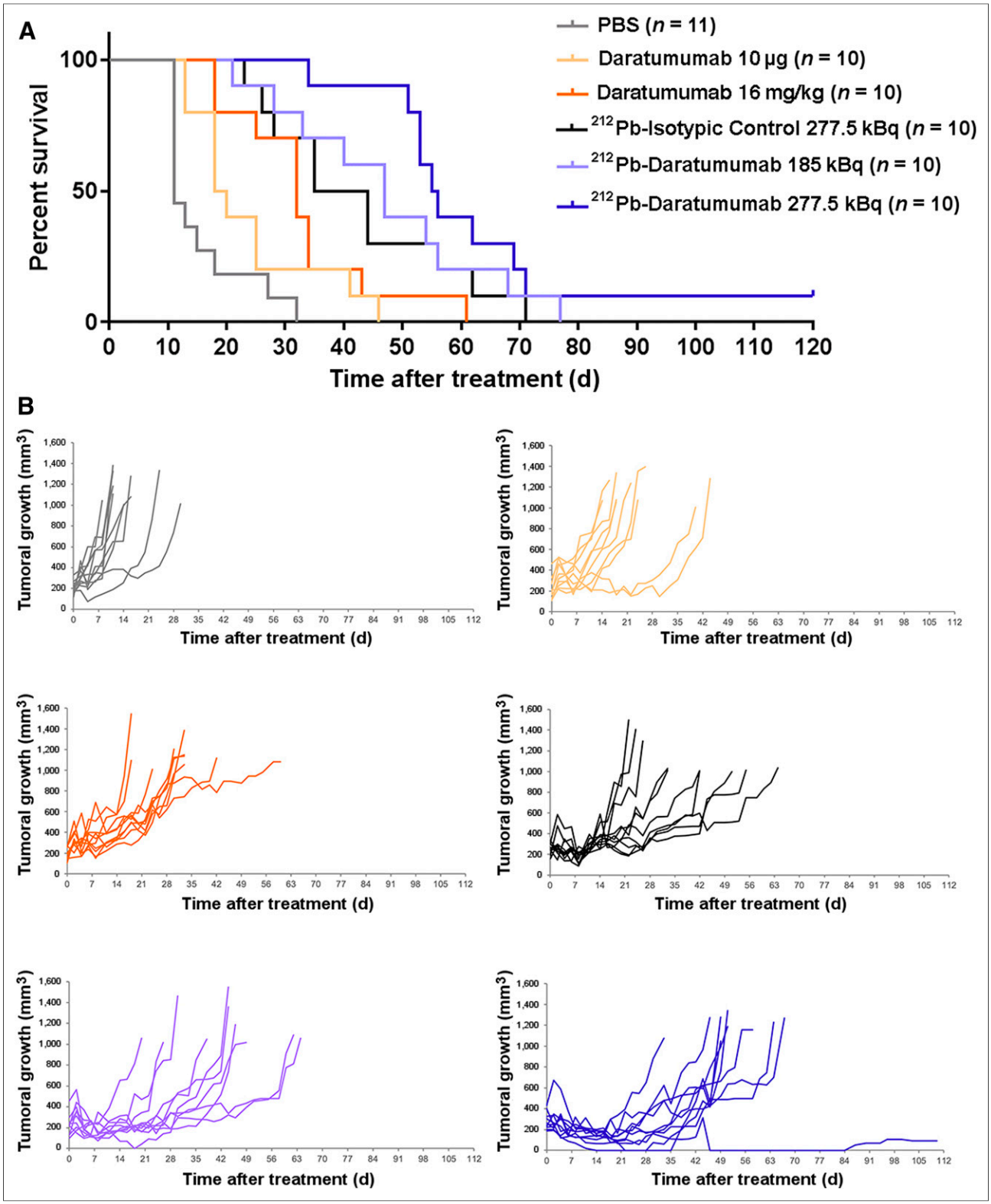

FIGURE 7. Efficacy of ^{212}Pb-daratumumab treatment on Rag2$^{-/-}\gamma C^{-/-}$ bearing subcutaneous xenograft of MM cells. Thirteen days after engraftment, mice received PBS, daratumumab (10 µg or 16 mg/kg), ^{212}Pb-isotypic control (277.5 kBq), or ^{212}Pb-daratumumab (185 or 277.5 kBq). (A) Kaplan–Meier survival analysis. Data were analyzed with log-rank test. (B) Individual tumoral growth evolution. Tumor volume was measured 3 times per week. Mice were euthanized when tumors were ≥1 cm^3 or when 120 d of survival was reached (end of experiment).

studies confirmed the pertinence of targeting CD38 in the treatment of MM (*17,18*).

Most MM RIT studies have used α-emitters. In fact, because MM cells are found either isolated in bone marrow or in small clusters, α-particles have a theoretic advantage over β-particles because of their high-linear-energy transfer and shorter range of action. Cell destruction would be more selective and irradiation less harmful to adjacent cells (*19*). As anticipated, a study of an anti-CD138 coupled with either ^{213}Bi or ^{177}Lu revealed the advantages of α-RIT over β-RIT in the treatment of MM in a preclinical model (*20*). Unfortunately, the fact that ^{213}Bi is a short-lived α-emitter (45 min) hampers its use in therapy. We chose to evaluate the α-emitter ^{212}Pb, selected for its longer half-life (10.6 h), which is more suitable with regard to antibody kinetics.

In this study, in vitro experiments showed ^{212}Pb-daratumumab–specific effects on proliferation of cells with high CD38 expression, as is consistent with previous observations by Teiluf et al. on different MM cell lines, including RPMI8226. Treatment with ^{213}Bi-anti-CD38 for 48 h induced a 50% lethal dose of 185 kBq/mL (*21*). In our experiment, the 50% lethal dose was 0.370 kBq/mL with 4 d of incubation. The high superior efficacy of ^{212}Pb when compared with ^{213}Bi correlates with its longer half-life as observed by Milenic et al., who compared the effects of ^{212}Pb and ^{213}Bi on human carcinoma cell line growth: concentrations needed to reach the same level of efficiency were 30–40 times lower for ^{212}Pb than for ^{213}Bi (*22*).

^{212}Pb-daratumumab biodistributions in mice bearing CD38-positive tumors are consistent with prior published data on ^{89}Zr-labeled daratumumab (*23,24*). We observed a specific tumor uptake that rapidly increased with time after injection, to reach 15 %ID/g at 18 h and 20–25 %ID/g at 48 h. Imaging data underlined a peripheral tumor fixation on large tumors, suggesting that small lesions might be the best indication for ^{212}Pb-RIT or RIT in general (our first idea) because of the slow tumor penetration of full-length antibodies in large tumors. Some uptake was observed in liver, spleen, kidney, and lung (~10 %ID/g), whereas uptake was minimal in other healthy tissues. Blood activity rapidly decreased and was around 20 % ID/g after 18 h.

Because of the low ^{212}Pb activity injected and the detection sensitivity, whole-body SPECT/CT images using ^{212}Pb-mAbs could not be acquired and were therefore performed with ^{203}Pb. This radioelement allowed us to consider a theranostic approach for ^{212}Pb α-therapy with a chemically identical radiometal, preventing the need for a radionuclide with different physical–chemical properties that would likely result in different pharmacokinetics. Imaging with ^{203}Pb could provide an effective approach to optimize therapeutic doses using patient-specific dosimetry calculations and to monitor patient response to targeted radionuclide therapy with ^{212}Pb.

Because daratumumab does not bind to mCD38, mCD38 biodistribution and toxicity studies were evaluated with a specific anti-mCD38 mAb. Human CD38 and mouse CD38 share sequence homology (70%) but display a different expression pattern, particularly among lymphocyte subsets and within the B-lineage (*25*). Murine CD38 is expressed abundantly by all murine B-lineage cells; by contrast, human CD38 is expressed highly by germinal center human B cells and less intensely by other human B-lineage cells. This expression pattern explains the high spleen uptake of ^{212}Pb-anti-mCD38 in mice. ^{212}Pb-anti-mCD38 biodistribution studies predicted the spleen and liver to be the dose-limiting normal organs; however, the differences in expression patterns limit elemental transposition to human ^{212}Pb-daratumumab toxicity.

Hematologic toxicity was studied through blood cell counts and flow cytometry on lymphoid organs after death. We observed a reversible hematologic toxicity similar to that observed by Boudousq et al. with ^{212}Pb-trastuzumab and ^{212}Pb-irrelevant mAb in intraperitoneal tumor xenograft–bearing nude mice (*26*). In parallel, we investigated toxicity in the liver and kidneys using a chemical approach. Consistent with the studies of Chérel et al. on ^{213}Bi-anti-mCD138, we observed no variations in liver or kidney enzymes in our acute toxicity study (*15*).

No toxicity was observed with ^{212}Pb-daratumumab up to 370 kBq because of the lack of cross-reactivity with mCD38. Nevertheless, considering the ^{212}Pb-anti-mCD38 toxicity outcome, for this first efficacy study we chose to test an activity of 277.5 kBq to remain under toxic ^{212}Pb-anti-mCD38 activities (370 kBq). In clinical application, injection of cold mAb before RIT could be an attractive option to optimize the therapeutic effect and reduce toxicity.

Efficacy studies were conducted on Rag2$^{-/-}\gamma C^{-/-}$ mice bearing RPMI8226 cell-line xenografts. In vitro results warranted the use of this cell line as a relevant xenograft model for in vivo studies. Treatment with ^{212}Pb-mAbs significantly reduced tumor growth and prolonged median survival compared with cold daratumumab or PBS. A significant partial efficacy was obtained with ^{212}Pb-isotypic control (277.5 kBq), corresponding to the effect of nontargeted RIT, likely because of the enhanced permeability and retention effect in tumors, observed in various studies with ^{212}Pb or other radioelements (*27*). In a single treatment regimen on a relatively high tumor volume at treatment time, the significantly greater inhibition of tumor growth observed with ^{212}Pb-daratumumab is encouraging, especially considering the relatively low activities used compared with other studies (*27*).

CONCLUSION

These promising results highlight the potency of ^{212}Pb-daratumumab in the treatment of MM. The ^{212}Pb half-life of 10.6 h, its central production, and its worldwide distribution provide clinical feasibility. To further optimize the effectiveness of ^{212}Pb-daratumumab, a fractionated regimen could be tested to improve the long-term efficacy of the therapy and prevent tumoral recurrence.

DISCLOSURE

This research was supported by BPI France. Amal Saidi is an Orano Med employee. No other potential conflict of interest relevant to this article was reported.

ACKNOWLEDGMENTS

We thank François Dalmay for assistance with the statistical analyses and Tania Stallons for English corrections.

KEY POINTS

QUESTION: What is the potential of ^{212}Pb-daratumumab in the treatment of plasma cell malignancies?

PERTINENT FINDINGS: In a single treatment regimen, ^{212}Pb-daratumumab induced significant tumor growth inhibition.

IMPLICATIONS FOR PATIENT CARE: ^{212}Pb-daratumumab could be promising in MM treatment.

REFERENCES

1. Abramson HN. The multiple myeloma drug pipeline—2018: a review of small molecules and their therapeutic targets. *Clin Lymphoma Myeloma Leuk.* 2018;18: 611–627.
2. Witzig TE. Radioimmunotherapy for B-cell non-Hodgkin lymphoma. *Best Pract Res Clin Haematol.* 2006;19:655–668.
3. Baidoo KE, Yong K, Brechbiel MW. Molecular pathways: targeted α-particle radiation therapy. *Clin Cancer Res.* 2013;19:530–537.
4. Kim Y-S, Brechbiel MW. An overview of targeted alpha therapy. *Tumour Biol.* 2012;33:573–590.
5. Yong K, Brechbiel MW. Towards translation of ^{212}Pb as a clinical therapeutic: getting the lead in! *Dalton Trans.* 2011;40:6068–6076.
6. Chappell LL, Ma D, Milenic DE, et al. Synthesis and evaluation of novel bifunctional chelating agents based on 1,4,7,10-tetraazacyclododecane-N,N′,N″,N‴-tetraacetic acid for radiolabeling proteins. *Nucl Med Biol.* 2003;30:581–595.
7. Meredith RF, Torgue J, Azure MT, et al. Pharmacokinetics and imaging of ^{212}Pb-TCMC-trastuzumab after intraperitoneal administration in ovarian cancer patients. *Cancer Biother Radiopharm.* 2014;29:12–17.
8. Meredith RF, Torgue JJ, Rozgaja TA, et al. Safety and outcome measures of first-in-human intraperitoneal α radioimmunotherapy with ^{212}Pb-TCMC-trastuzumab. *Am J Clin Oncol.* 2018;41:716–721.
9. Deaglio S, Aydin S, Vaisitti T, Bergui L, Malavasi F. CD38 at the junction between prognostic marker and therapeutic target. *Trends Mol Med.* 2008;14: 210–218.
10. Bataille R, Jégo G, Robillard N, et al. The phenotype of normal, reactive and malignant plasma cells: identification of "many and multiple myelomas" and of new targets for myeloma therapy. *Haematologica.* 2006;91:1234–1240.
11. de Weers M, Tai Y-T, van der Veer MS, et al. Daratumumab, a novel therapeutic human CD38 monoclonal antibody, induces killing of multiple myeloma and other hematological tumors. *J Immunol.* 2011;186:1840–1848.
12. Carpenet H, Cuvillier A, Monteil J, Quelven I. Anti-CD20 immunoglobulin G radiolabeling with a ^{99m}Tc-tricarbonyl core: in vitro and in vivo evaluations. *PLoS One.* 2015;10:e0139835.
13. van de Donk NWCJ, Janmaat ML, Mutis T, et al. Monoclonal antibodies targeting CD38 in hematological malignancies and beyond. *Immunol Rev.* 2016;270: 95–112.
14. Donís-Hernández FR, Parkhouse RME, Santos-Argumedo L. Ontogeny, distribution and function of CD38-expressing B lymphocytes in mice. *Eur J Immunol.* 2001;31:1261–1267.
15. Chérel M, Gouard S, Gaschet J, et al. ^{213}Bi radioimmunotherapy with an anti-mCD138 monoclonal antibody in a murine model of multiple myeloma. *J Nucl Med.* 2013;54:1597–1604.
16. Morandi F, Horenstein AL, Costa F, Giuliani N, Pistoia V, Malavasi F. CD38: a target for immunotherapeutic approaches in multiple myeloma. *Front Immunol.* 2018;9:2722.
17. Green DJ, Orgun NN, Jones JC, et al. A preclinical model of CD38-pretargeted radioimmunotherapy for plasma cell malignancies. *Cancer Res.* 2014;74:1179–1189.
18. Green DJ, O'Steen S, Lin Y, et al. CD38-bispecific antibody pretargeted radioimmunotherapy for multiple myeloma and other B-cell malignancies. *Blood.* 2018;131:611–620.
19. Chatterjee M, Chakraborty T, Tassone P. Multiple myeloma: monoclonal antibodies-based immunotherapeutic strategies and targeted radiotherapy. *Eur J Cancer.* 2006;42:1640–1652.
20. Fichou N, Gouard S, Maurel C, et al. Single-dose anti-CD138 radioimmunotherapy: bismuth-213 is more efficient than lutetium-177 for treatment of multiple myeloma in a preclinical model. *Front Med (Lausanne).* 2015;2:76.
21. Teiluf K, Seidl C, Blechert B, et al. α-radioimmunotherapy with ^{213}Bi-anti-CD38 immunoconjugates is effective in a mouse model of human multiple myeloma. *Oncotarget.* 2015;6:4692–4703.
22. Milenic DE, Garmestani K, Brady ED, et al. Alpha-particle radioimmunotherapy of disseminated peritoneal disease using a ^{212}Pb-labeled radioimmunoconjugate targeting HER2. *Cancer Biother Radiopharm.* 2005;20:557–568.
23. Kang L, Jiang D, England CG, et al. ImmunoPET imaging of CD38 in murine lymphoma models using ^{89}Zr-labeled daratumumab. *Eur J Nucl Med Mol Imaging.* 2018;45:1372–1381.
24. Ghai A, Maji D, Cho N, et al. Preclinical development of CD38-targeted [^{89} Zr]Zr-DFO-daratumumab for imaging multiple myeloma. *J Nucl Med.* 2018;59:216–222.
25. Lund F, Solvason N, Grimaldi JC, Michael R, Parkhouse E, Howard M. Murine CD38: an immunoregulatory ectoenzyme. *Immunol Today.* 1995;16:469–473.
26. Boudousq V, Bobyk L, Busson M, et al. Comparison between internalizing anti-HER2 mAbs and non-internalizing anti-CEA mAbs in alpha-radioimmunotherapy of small volume peritoneal carcinomatosis using ^{212}Pb. *PLoS One.* 2013;8: e69613.
27. Kasten BB, Gangrade A, Kim H, et al. ^{212}Pb-labeled B7-H3-targeting antibody for pancreatic cancer therapy in mouse models. *Nucl Med Biol.* 2018;58:67–73.

Results of the first clinical trial on targeted alphatherapy with lead-212

OPEN

Safety and Outcome Measures of First-in-Human Intraperitoneal α Radioimmunotherapy With ^{212}Pb-TCMC-Trastuzumab

Ruby F. Meredith, MD, PhD, Julien J. Torgue, PhD,† Tania A. Rozgaja, PhD,† Eileen P. Banaga, MS,† Patty W. Bunch, OCN,‡ Ronald D. Alvarez, MD,‡ J. Michael Straughn Jr, MD,‡ Michael C. Dobelbower, MD, PhD,* and Andrew M. Lowy, MD§*

Purpose: One-year monitoring of patients receiving intraperitoneal (IP) ^{212}Pb-TCMC-trastuzumab to provide long-term safety and outcome data. A secondary objective was to study 7 tumor markers for correlation with outcome.

Methods: Eighteen patients with relapsed intra-abdominal human epidermal growth factor receptor-2 expressing peritoneal metastases were treated with a single IP infusion of ^{212}Pb-TCMC-trastuzumab, delivered <4 h after 4 mg/kg IV trastuzumab. Seven tumor markers were studied for correlation with outcome.

Results: Six dose levels (7.4, 9.6, 12.6, 16.3, 21.1, 27.4 MBq/m^2) were well tolerated with early possibly agent-related adverse events being mild, transient, and not dose dependent. These included asymptomatic, abnormal laboratory values. No late renal, liver, cardiac, or other toxicity was noted up to 1 year. There were no clinical signs or symptoms of an immune response to ^{212}Pb-TCMC-trastuzumab, and assays to detect an immune response to this conjugate were negative for all tested. Tumor marker studies in ovarian cancer patients showed a trend of decreasing Cancer antigen 72-4 (CA 72-4) aka tumor-associated glycoprotein 72 (TAG-72) and tumor growth with increasing administered radioactivity. Other tumor markers, including carbohydrate antigen (CA125), human epididymis protein 4 (HE-4), serum amyloid A (SAA), mesothelin, interleukin-6 (IL-6), and carcinoembryonic antigen (CEA) did not correlate with imaging outcome.

Conclusions: IP ^{212}Pb-TCMC-trastuzumab up to 27 MBq/m^2 seems safe for patients with peritoneal carcinomatosis who have failed standard therapies. Serum TAG-72 levels better correlated to imaging changes in ovarian cancer patients than the more common tumor marker, CA125.

Key Words: Pb-212-radioimmunotherapy, cancer, ovarian, tumor marker, intraperitoneal

(*Am J Clin Oncol* 2018;41:716–721)

From the Departments of *Radiation Oncology; ‡Gynecology, Comprehensive Cancer Center, University of Alabama at Birmingham, Birmingham, AL; †AREVA Med, Plano, TX; and §Department of Surgery, Division of Surgical Oncology, Moores Cancer Center, University of California, San Diego, CA.

Supported by AREVA Med and NIH CCTS grant 1UL1TR001417.

J.J.T., T.A.R., and E.P.B. are AREVA Med employees. R.F.M. joined the Scientific Advisory Board July 2015. The other authors declare no conflicts of interest.

Reprints: Ruby F. Meredith, MD, PhD, Hazelrig Salter Radiation Oncology Center, 1700 6th Ave. South, 176 F, Birmingham, AL, 35249. E-mail: lobrown@uabmc.edu.

ISSN: 0277-3732/18/4107-0716

DOI: 10.1097/COC.0000000000000353

Low toxicity intraperitoneal (IP) treatment continues to be an unmet need for disease that spreads through the cavity such as ovarian and pancreatic cancer. IP chemotherapy has improved survival of ovarian cancer patients but carries risk of life-threatening toxicity, and has not become the standard at most institutions.[1] Radiopharmaceuticals have greater potential than external beam radiation due to dose-limiting tolerance of normal organs. β-emitting radiopharmaceuticals have shown modest impact but have also been used at dose-limiting toxicity levels.[2–5] Targeted α-emitter radiopharmaceuticals, as implemented in this report, have the potential advantages of improved efficacy with less toxicity than β-emitters.

For targeted radionuclide therapy, the high ionization density of α-particles is attractive but their development/implementation has been challenging compared with the more widely available β-emitters.[6,7] With the large helium particle emitted, α-decay results in significantly higher energy delivery (linear energy transfer) than β-decay, which results in higher cell-killing effectiveness. Human cell culture studies showed the relative biological effectiveness (RBE) greater for α-particles than that for β-radiation or kilovoltage photons[8]; this has been confirmed in other preclinical as well as early clinical trials but the RBE range has been variable from ∼1 to 20.[9] The clinical experience where ^{213}Bi-HuM195 and ^{90}Y-HuM195 therapy could be directly compared in leukemic patients suggested that the RBE of α-emitter therapy will vary with cell type, geometry, and endpoints utilized.[10] Another advantage of α-particles over β-radiation is the limited range of only a few cell diameters. This spares normal tissues but does limit optimal use to selected clinical applications. Appropriate clinical settings for use of high potency α-particles with short half-lives are those where the targeting is very specific and rapid or other conditions, such as into a resection cavity or tumor mass, where there is limited exposure to normal tissues. Because of many hurdles, implementation of systemic administration using antibody targeted α conjugates has been limited to a few studies, mainly in patients with leukemia, lymphoma, and metastatic melanoma.[7,11–13] Limited experience with nonsystemic administration has included intralesional melanoma sites, intracavity or intralesional for brain tumors, and intraperitoneal infusion.[14–18] Whereas reports of others show more extensive pharmacokinetics and dosimetry of another α-emitter conjugate administered to the peritoneal cavity (^{211}At-Mx35 F(Ab')$_2$), our following report is the first therapeutic IP administration where safety was the primary objective posttherapy.[16,18,19] Targeted α-conjugate therapy has thus far been well tolerated but initial dose levels have been modest to minimize risks to patients undergoing investigational treatment. This first-in-human clinical trial of IP ^{212}Pb-TCMC2-(4-isothiocyanobenzyl)-1,4,7,10-teraaza-1,4,7,10-tetra-(2-carbamonyl methyl)-cyclododecane-trastuzumab was initiated after extensive murine and nonhuman

primate investigations provided biodistribution, safety, and antitumor efficacy data.[20–24] In this phase I study, a single IP infusion of ^{212}Pb-TCMC-trastuzumab was escalated over 6 dose levels with toxicity monitoring to confirm the safety of this agent.

This trial, like many other investigations, studied serum tumor markers as indicators of therapeutic efficacy that could be easily and quickly monitored. This is particularly relevant given the limitations inherent in image-based quantification of peritoneal metastatic disease. Seven tumor markers were studied for their correlation to clinical outcome 6 weeks posttherapy. These included carcinoembryonic antigen (CEA), which is used for monitoring patients with gastrointestinal cancer and a minority of patients with other malignancies.[25] Carbohydrate antigen (CA125) was monitored in the ovarian cancer patients as this has historically been the standard marker for monitoring of disease response to treatment.[26–29] Human epididymis protein 4 (HE-4), serum amyloid A (SAA), mesothelin, interleukin-6 (IL-6), and tumor-associated glycoprotein (TAG-72), were also chosen for study based on prior reports of tumor association.[30–36]

METHODS

Details of the trial design and agent preparation have been previously reported.[17] Briefly, this trial provided a single IP ^{212}Pb-TCMC-trastuzumab infusion <4 h after 4 mg/kg IV trastuzumab in patients with human epidermal growth factor receptor-2 (HER-2) expressing malignancy that had failed standard therapies. Modifications were made after patient 10 to allow patients with HER-2 of 1+ in ≥10% of cells. Modification was also made to discontinue the saturated solution of potassium iodide as imaging showed no thyroid localization and no abnormal laboratory values had been observed in >1 year for the initial 3 patients. The diuretic regimen was also shortened as there was no evidence of renal localization or toxicity and patients had difficulty with side effects such that most were noncompliant with the entire prescribed regimen. Monitoring over the duration of 1 year included clinical findings, laboratory values, cardiac studies, immunologic assays, serum tumor marker levels, and computed tomographic scans. Patients had clinical and/or laboratory posttherapy evaluations 7 times in the first 6 weeks. If there was no toxicity, scheduled monitoring was extended to 6-, and then to 12-week intervals. Cardiac monitoring used electrocardiogram and echocardiograms. Enzyme linked immunosorbent assay testing of 6-week serum samples was performed to determine if there was any evidence of an immune response to TCMC-trastuzumab. A standard anti-drug antibody assay was developed. Briefly, the anti-Her-2 antibody was both the coat and a biotinylated primary detection antibody. Patient serum or polyclonal antibodies raised against TCMC-trastuzumab was the analyte. In the presence of bivalent anti TCMC-trastuzumab antibodies, the biotinylated trastuzumab antibody becomes linked to the trastuzumab coat. HRP-streptavidin is then added to develop a signal. Toxicity was defined using Common Terminology Criteria for Adverse Events (version 4.03 National Cancer Institute). Imaging interpretation and lesion measurements from baseline (<4 w pretreatment) and 6-week interval posttreatment CT scans were performed as an independent review by Imaging Endpoints (Scottsdale, AZ). Lesion measurements were compared by pretreatment and posttreatment volumes as a modification from RECIST criteria described in the original study design that uses tumor diameter products.[37] Levels of standard tumor markers CA125 and CEA were obtained at institution laboratories; commercially available kits were used for other markers HE-4 (Fujirebio Diagnostics Inc., in vitro diagnostics), Cancer antigen (CA 72-4) (TAG-72) (DRG International, Research Use Only), SAA (Life Technologies, Ruo), Mesothelin (Aviscera Bioscience Inc., Ruo), IL-6 (Abcam, Ruo). Serum for tumor markers was obtained pretreatment, at 6 weeks, and at additional timepoints for CEA and CA125 in most patients. Statistical analysis used least squares linear regression to fit the data.

RESULTS

Toxicity

Eighteen patients (age 46 to 83) treated at 6 dose levels (7.4, 9.6, 12.6, 16.3, 21.1, 27.4 MBq/m^2) were monitored for at least 1 year or until death. Seventeen patients were treated at the University of Alabama at Birmingham, and 1 colon cancer patient was treated at the University of California at San Diego. Sixteen patients were females with ovarian cancer and 2 males had colon cancer. Treatment was well tolerated. Mild acute adverse effects were associated with the investigational agent as previously presented for the initial 16 patients.[18] Other than 2 patients who had transient abdominal pain associated with agent plus saline administration, possibly related adverse events were mainly grade 1, transient, asymptomatic laboratory abnormalities that were not dose related.

The patients are numbered 1 to 18 by the order of treatment. Monitoring of the enzymes lactic dehydrogenase (LDH), alkaline phosphatase (AlkP), alanine aminotransferase (ALT), aspartate aminotransferase (AST), and γ glutamyltransferase (GGT) showed no elevation among patients 2, 3, 7, 8, 12, 15, 16, 17, and 18. Table 1 shows the time and frequency of patients who developed grade 1 liver function test elevations. As shown in Table 1, 4 patients had elevations before treatment and 6 others experienced elevation to grade 1 level after treatment. These minor fluctuations did not appear dose related; all except patient 14 were below dose level 5 and none occurred at the highest dose level.

TABLE 1. Summary of Enzyme Abnormalities by Date

	Patients With Enzyme Elevations				
Week After Treatment	**LDH**	**AlkP**	**ALT**	**AST**	**GGT**
Pretreatment	4, 5	1, 10		5	
Week 1	4, 5, 6	1, 9, 14	11	5, 11	5
Week 4	4	1			
Week 6	4	1, 14	14	13, 14	14

Each patient number is used for all times of grade 1 enzyme elevation from pretreatment to week 6.
AlkP indicates alkaline phosphatase; ALT, alanine aminotransferase; AST, aspartate aminotransferase; GGT, γ glutamyltransferase; LDH, lactic dehydrogenase.

Whereas hematologic toxicity has been dose-limiting in prior IP radionuclide conjugate studies, the mean platelet counts, total white blood cell counts, and neutrophil counts remained normal after a mean equivalent dose to marrow of 0.002 to 0.14 cGy/MBq. Only 2 patients had transient decreased counts to grade 1 (platelets 142,000/μL, WBC 3500/μL without neutropenia). Anemia was not tracked for toxicity as 6 patients were anemic pretreatment with hemoglobin of 9.8 to 11.2 g/dL. The percent change at 6 weeks for these patients was from a loss of 3.8% to a gain of 16.3%. Three of the 6 had improvement to normal hemoglobin levels during that interval.

Four patients experienced periods of grade 1 creatinine elevation (without proteinuria) associated with dehydration or urinary tract obstruction as reported.[18] Reducing the diuretic regimen after patient 10 did not increase the serum levels of radioactivity or result in renal toxicity. No late renal, liver, hematologic (excluding anemia as noted above), cardiac, or other toxicity has been observed with monitoring >1 year despite additional therapy after the investigational agent. Although all patients had disease progression in <8 months and proceeded with additional treatment, none refused continued monitoring. There were no clinical signs or symptoms of an immune response, and assays to detect an immune response to ^{212}Pb-TCMC-trastuzumab were negative for all 15 of 15 tested (3 patients had no sample).

Tumor Marker Changes Compared With Clinical Response

Blood levels of 7 tumor markers were studied and compared with clinical outcome at 6 weeks posttherapy. CEA and CA125 continued to be obtained until progression. CEA increased with disease progression in the 2 colon cancer patients but all the ovarian cancer patients had levels that were within the normal range both pretreatment and posttreatment. Other tumor markers which are often associated with ovarian cancer, including CA125, mesothelin, IL-6, SAA, and HE-4, did not correlate with imaging outcome (Fig. 1). Only a TAG-72 had a pattern similar to that of tumor growth changes. TAG-72 levels covered a wide range from nearly 200% increase to 66% decrease 6 weeks posttherapy. Compared with the imaging changes, the TAG-72 pattern had a steeper slope and higher correlation coefficient with administered level of radioactivity than did tumor growth (R^2 for TAG-72 is 0.73 vs. 0.21 for CT) as shown in Figure 2. Five patients did not have measurable tumor lesions (TL) and are not included in Figure 2. Their clinical outcome is included in Table 2, which shows a trend of less tumor growth, including regression, with increasing administered radioactivity. All patients had progression of disease inside and/or outside of the peritoneal cavity before 8 months but the majority lived >1 year, allowing monitoring for late toxicity.

DISCUSSION

The single IP ^{212}Pb-TCMC-trastuzumab infusion was well tolerated with agent-related toxicities limited to grade 1 and the majority of them were asymptomatic, transient laboratory abnormalities. Although there was no visualization of radioactivity outside of the peritoneal cavity, blood collection showed a rate of <1% to 22.9% transit in 24 hours.[18] The imaging and blood data allowed dosimetry calculations. These found low radiation exposure to normal organs and a mean tumor milieu to marrow ratio of >1000, as most of the radioactivity decay took place in the peritoneal fluid.[17]

With >1 year of follow-up in the majority of patients receiving IP ^{212}Pb-TCMC-trastuzumab, no late toxicity has been observed. The paucity of preclinical toxicity data allowed dose escalation for 6 levels, which is the maximum that was planned for this first-in-human study; further increase in dose levels would have soon exceeded preclinical data and required additional nonhuman primate studies.[38] On the basis of this initial clinical experience, ^{212}Pb-TCMC-trastuzumab appears safe for further study at the highest dose level tested or even additional dose escalation. As IP α-emitter therapy should be most effective for microscopic disease, the low toxicity should allow it to be further studied in combination with other agents or as an adjuvant after tumor reduction by standard therapies. The transient early toxicities did not appear to be dose related. The grade 1 leukopenia and thrombocytopenia occurred in patients at dose groups 3 and 5. No drops in blood counts to grade 1 were noted in the highest dose group, suggesting

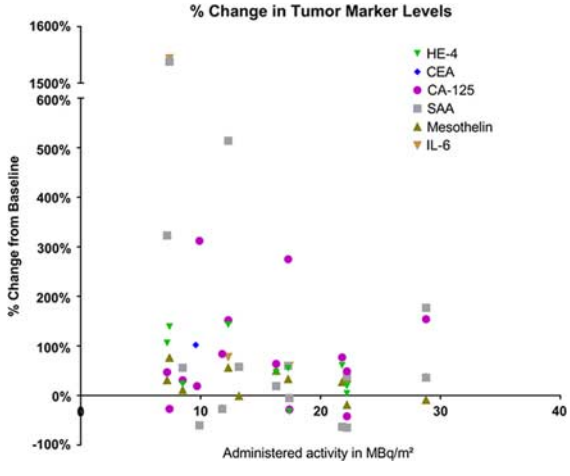

FIGURE 1. Each data point represents the increase or decrease in serum marker as percent change at 6 weeks compared with baseline for individual patients. The change in markers is compared with administered radioactivity in MBq/m^2. Data points are not shown when values were within normal limits.

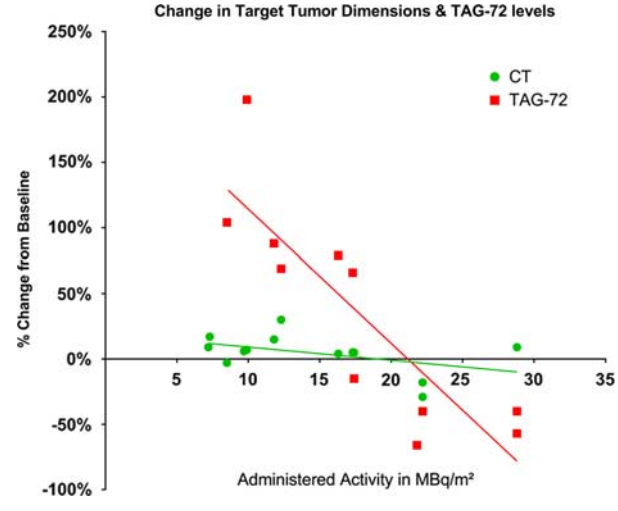

FIGURE 2. Each data point represents a single patient who had measureable lesions and TAG-72 >6 U/mL at baseline. The data points are expressed as percent change from baseline. The lines represent best fit from regression analysis. TAG-72 indicates tumor-associated glycoprotein 72.

TABLE 2. Comparison of Posttreatment Disease Status With Administered ^{212}Pb Dose Level

Patient #	6 wks post-dose	12 wks post-dose	24 wks post-dose	Dose (mCi/m^2)	Comments
1	PD			0.2	PD due to ascites
2	SD	PD		0.2	PD due to non-TLs and ascites
3	PD			0.2	no TLs; PD due to ascites
4	PD			0.26	New ascites
5	PD			0.26	PD due to non-TLs
6	PD			0.26	PD due to ascites at 5wk
8	PD			0.26	new lesion at 6 wks
7	PD			0.34	PD due to non-TLs
9	PD			0.34	PD due to TL and non-TL and ascites
10	SD	PD	PD	0.34	no TLs, new lesion at 12 wks
11	SD/NC+	SD/NC+		0.44	PD at 21 wks
12	SD/NC+	PD		0.44	PD due to TL & non-TLs
13	SD/NC+	PD		0.44	PD due to non-TLs and ascites
14	SD	SD		0.57	PD pleural effusion 12 wk
15	SD/MR	SD/MR	SD	0.57	New TL outside abdomen 30wk
16	SD/MR	SD/MR		0.57	Clinical PD 14 wk
17	SD	SD	PD	0.74	PD at 24 wks due to ascites increase
18	SD/NC+	PD		0.74	Progression in TL

PD	Progressive Disease: Measureable tumor lesions (TL) > 20% increase, new lesions or clinical progression of non TL
SD	Stable Disease: No change (NC) that qualifies as progression or response.
SD/NC-	Stable Disease/ NC-: 0% to 10% reduction
SD/NC+	Stable Disease/ NC+: 0% to 20% increase
SD/MR	Stable Disease/ Minor Response (MR): >20% reduction of TL.
ND	No diagnostic images at that time (ND).

The most current computed tomographic scan measurements were compared with baseline scan measurements using a modified RECIST 1.1.

factors other than radiation dose alone were associated with the count levels posttherapy. Both of the affected patients had pretreatment levels of only 12% above the lower limits of normal such that a modest drop reached grade 1 level. As the radiation dose to marrow was small at 0.002 to 0.14 cGy/MBq, significant hematologic toxicity would not be expected and was not observed.[18] Six of 16 ovarian cancer patients were anemic pretherapy and 3 had improvement to normal levels even during the initial 6 weeks posttherapy. The early post-treatment increase of hemoglobin would not have been expected with higher, marrow-toxic, doses of radiation and suggests incomplete recovery from toxicities of therapy before administration of this investigational agent.

Both methods of index lesion measurement, individual volume versus sum of lesion diameter products, showed a trend of less tumor growth with increasing level of administered radioactivity. The independent review shows more early patients with progression than previously noted when pretreatment and posttreatment comparison used the product of index lesion diameter (Table 2).[17,37] However, the later independent review did not necessarily use the same index lesions, which contributed to less than complete concordance of tumor growth results from those previously reported.[17] Although the optimal tumor efficacy with α-emitters is proposed to be for microscopic disease, regression was noted among various sized gross lesions.

Many investigators continue to seek serum tumor markers to facilitate diagnosis and monitoring of therapeutic efficacy. Although CA125 has become the standard marker for monitoring antitumor effects in ovarian cancer, checking this alone has not been rigorous enough to become a standard for diagnostic screening.[39] Its use in conjunction with other serum markers, plus additional factors, has been more helpful.[30,40] Other potential markers under study for ovarian cancer include IL-6, IL-8, kallikrein-10, mesolthelin, HE-4, and p53.[41–44] Also, SAA may be useful in serous subtype of ovarian carcinoma.[45]

In this study, several tumor markers were monitored to determine their potential utility for noninvasive assessment of therapeutic response. Although levels of the standard ovarian cancer tumor marker CA125 did not have a strong relation to outcome, CA125 may have been a better marker had the

pretreatment level been obtained closer to the time to treatment. With the measures of this noncancer specific protein usually 2 to 4 weeks before therapy plus intervening manipulation of the peritoneal cavity with catheter insertion and treatment, the posttreatment levels may have been elevated by factors other than tumor burden. One might expect that elevation related to disruption by catheter placement and therapy would have resolved by 6 weeks but further study would be needed to seek relevant information for this determination.

HE-4 has also been studied as a tumor marker of ovarian cancer. It has been more helpful for diagnosis than for monitoring therapeutic response. HE-4 has most frequently been used in conjunction with CA125 and other factors to distinguish ovarian cancer from a benign abdominal process.[40,46,47] The mucin-like TAG-72 is generally expressed on adenocarcinomas and less frequently in other types of malignancies.[48–50] The only normal tissue with notable TAG-72 expression is secretory endometrium, which was not of concern in this study as none of the patients had an intact uterus.[49,50] Tumor shedding of TAG-72 is common and may allow potential noninvasive monitoring of tumor status via blood levels,[49] with the assumption that it correlates with tumor burden in an individual patient. TAG-72 had the strongest correlation with CT-monitored tumor changes of the 7 markers reported here. None of the other markers tested showed a good correlation with increasing radioactivity or clinical outcome. Although they have all been associated with ovarian cancer, CA125 is the only marker robust enough to routinely be used and it is not cancer specific. TAG-72 had a relatively robust association with increasing administered radioactivity, having a correlation coefficient of 0.73. On the basis of that, plus its decreasing trend with decreasing tumor growth, a dose/response relation with administered radioactivity is suggested. Additional data are needed to confirm this and to further investigate TAG-72 as a serum marker of response to ^{212}Pb-TCMC-trastuzumab. CEA is a serum marker used as a standard in monitoring response to therapy in colon/rectal cancer. We found it was helpful in the 2 colon cancer patients in this study. CEA may be elevated, and thus is a potential marker for monitoring other gastrointestinal malignancies as well other malignancies of nongastrointestinal origin albeit in a smaller fraction of patients. In this study, all the ovarian cancer patients had normal CEA levels pretreatment and none experienced elevated levels at follow-up, even when disease progression was noted from imaging and other markers (TAG-72).

CONCLUSIONS

IP ^{212}Pb-TCMC-trastuzumab up to 27.4 MBq/m^2 appears safe for further study and dose escalation. Serum TAG-72 monitoring is recommended as a potential tumor marker for assessing antitumor effects in patients with ovarian cancer.

ACKNOWLEDGMENTS

The authors thank many for conduct of this study that required an international team: J. Maxwell Austin, Souheil Saddekni, Jacob Estes, Andres Forero, Melissa Baird, Charles Leath, III, Mack Barnes, Desiree Morgan, the late Michael Azure, Jinda Fan, Denise Charlotte Jeffers, Sui Shen, Darrell Fisher, Brenda Sandmaier, Olivier Rixe, Kurt Zinn, Ronda Carlise, Alma Del Grosso, Rebecca Quinn, Robert Oster, Rusty Caranto, Daniel Yoder, Lolinda Brown, Martin Brechbiel, Shakeela Dad, Debbie Soldano, Paul Fanta, Thelma Webb, and Brandy Jonas.

REFERENCES

1. Tewari D, Java JJ, Salani R, et al. Long-term survival advantage and prognostic factors associated with intraperitoneal chemotherapy treatment in advanced ovarian cancer: a gynecologic oncology group study. *J Clin Oncol*. 2015;33:1460–1466.
2. Stewart JS, Hird V, Sullivan M, et al. Intraperitoneal radioimmunotherapy for ovarian cancer. *BJOG*. 1989;96:529–536.
3. Meredith R, You Z, Alvarez R, et al. Predictors of long-term outcome from intraperitoneal radioimmunotherapy for ovarian cancer. *Cancer Biother Radiopharm*. 2012;26:36–40.
4. Vergote IB, Vergote-De Vos LN, Abeler VM, et al. Randomized trial comparing cisplatin with radioactive phosphorus or whole-abdomen irradiation as adjuvant treatment of ovarian cancer. *Cancer*. 1992;69:741–749.
5. Oei AL, Verheijen RH, Seiden MV, et al. Decreased intraperitoneal disease recurrence in epithelial ovarian cancer patients receiving intraperitoneal consolidation treatment with yttrium-90-labeled murine HMFG1 without improvement in overall survival. *Int J Cancer*. 2007;120:2710–2714.
6. Sgouros G, Roeske JC, McDevitt MR, et al. MIRD pamphlet no. 22 (abridged): radiobiology and dosimetry of {alpha}-particle emitters for targeted radionuclide therapy. *J Nucl Med*. 2010;51:311–328.
7. Elgqvist J, Frost S, Pouget JP, et al. The potential and hurdles of targeted alpha therapy—clinical trials and beyond. *Front Oncol*. 2014;3:324.
8. Barendsen GW. Dose-survival curves of human cells in tissue culture irradiated with alpha-, beta-, 20-kV. x- and 200-kV. X-radiation. *Nature*. 1962;193:1153–1155.
9. Allen BJBT, Brill AB, Fisher DR, et al. MIRD monograph—radiobiology and dosimetry for radiopharmaceutical therapy with alpha-particle emitters. *J Nucl Med*. 2015;56:1–63.
10. Sgouros GB, Shah WA, Watchman A, et al. Relative biological effectiveness for efficacy and toxicity in leukemia patients of the alpha-particle emitter, bismuth-213. *Cancer Biother Radiopharm*. 2006;21:397.
11. Jurcic JG, Larson SM, Sgouros G, et al. Targeted alpha particle immunotherapy for myeloid leukemia. *Blood*. 2002;100:1233–1239.
12. Allen BJ, Huang CY, Clarke RA. Targeted alpha anticancer therapies: update and future prospects. *Biologics*. 2014;8:255–267.
13. Jurcic JG, Ravandi F, Pagel JM, et al. Phase I trial of targeted alpha-particle immunotherapy with actinium-225-lintuzumab (anti-CD33) and low-dose cytarabine (LDAC) in older patients with untreated acute myeloid leukemia (AML). *Blood*. 2015;126:3794.
14. Zalutsky MR, Reardon DA, Akabani G, et al. Clinical experience with alpha-particle emitting 211At: treatment of recurrent brain tumor patients with 211At-labeled chimeric antitenascin monoclonal antibody 81C6. *J Nucl Med*. 2008;49:30–38.
15. Allen BJ, Raja C, Rizvi S, et al. Intralesional targeted alpha therapy for metastatic melanoma. *Cancer Biol Ther*. 2005;4:1318–1324.
16. Andersson H, Cederkrantz E, Back T, et al. Intraperitoneal {alpha}-particle radioimmunotherapy of ovarian cancer patients: pharmacokinetics and dosimetry of 211At-MX35 F(ab')2—a phase I study. *J Nucl Med*. 2009;50:1153–1160.
17. Meredith RF, Torgue J, Azure MT, et al. Pharmacokinetics and imaging of 212Pb-TCMC-trastuzumab after intraperitoneal administration in ovarian cancer patients. *Cancer Biother Radiopharm*. 2014;29:12–17.
18. Meredith RF, Torgue J, Shen S, et al. Dose escalation and dosimetry of first-in-human α radioimmunotherapy with 212 Pb-TCMC-trastuzumab. *J Nucl Med*. 2014;55:1636–1642.
19. Cederkrantz E, Andersson H, Bernhardt P, et al. Absorbed doses and risk estimates of (211)At-MX35 F(ab')2 in intraperitoneal therapy of ovarian cancer patients. *Int J Radiat Oncol Biol Phys*. 2015;93:569–576.
20. Azure MZK. *Intraperitoneal Injection Toxicity Study of 212Pb-TCMC-Trastuzumab in Cynomolgus Monkeys*. Birmingham: University of Alabama at Birmingham; 2010. contract No. AREVA01.
21. Milenic DE, Garmestani K, Brady ED, et al. Alpha-particle radioimmunotherapy of disseminated peritoneal disease using a

(212)Pb-labeled radioimmunoconjugate targeting HER2. *Cancer Biother Radiopharm*. 2005;20:557–568.
22. Milenic DE, Garmestani K, Brady ED, et al. Multimodality therapy: potentiation of high linear energy transfer radiation with paclitaxel for the treatment of disseminated peritoneal disease. *Clin Cancer Res*. 2008;14:5108–5115.
23. Milenic DE, Wong KJ, Baidoo KE, et al. Targeting HER2: a report on the in vitro and in vivo pre-clinical data supporting trastuzumab as a radioimmunoconjugate for clinical trials. *MAbs*. 2010;2:5, 1–15.
24. Milenic DE, Molinolo AA, Solivella MS, et al. Toxicological studies of 212Pb intravenously or intraperitoneally injected into mice for a phase 1 trial. *Pharmaceuticals*. 2015;8:416–434.
25. Lo Gerfo P, Krupey J, Hansen HJ. Demonstration of an antigen common to several varieties of neoplasia. *N Engl J Med*. 1971; 285:138–141.
26. Soletormos G, Duffy MJ, Othman Abu Hassan S, et al. Clinical use of cancer biomarkers in epithelial ovarian cancer: updated guidelines from the European Group on Tumor Markers. *Int J Gynecol Cancer*. 2016;26:43–51.
27. Bast RC Jr, Badgwell D, Lu Z, et al. New tumor markers: CA125 and beyond. *Int J Gynecol Cancer*. 2005;15(suppl 3):274–281.
28. Moss EL, Hollingworth J, Reynolds TM. The role of CA125 in clinical practice. *J Clin Pathol*. 2005;58:308–312.
29. Yurkovetsky Z, Skates S, Lomakin A, et al. Development of a multimarker assay for early detection of ovarian cancer. *J Clin Oncol*. 2010;28:2159–2166.
30. Kotowicz B, Fuksiewicz M, Sobiczewski P, et al. Clinical value of human epididymis protein 4 and the risk of ovarian malignancy algorithm in differentiating borderline pelvic tumors from epithelial ovarian cancer in early stages. *Eur J Obstet Gynecol Reprod Biol*. 2015;194:141–146.
31. Edgell T, Martin-Roussety G, Barker G, et al. Phase II biomarker trial of a multimarker diagnostic for ovarian cancer. *J Cancer Res Clin Oncol*. 2010;136:1079–1088.
32. Coticchia CM, Yang J, Moses MA. Ovarian cancer biomarkers: current options and future promise. *JNCCN*. 2008;6:795–802.
33. Qiao N, Li H. The value of mesothelin in the diagnosis and follow-up of surgically treated ovarian cancer. *Eur J Gynaecol Oncol*. 2013;34:163–165.
34. Anastasi E, Granato T, Falzarano R, et al. The use of HE4, CA125 and CA72-4 biomarkers for differential diagnosis between ovarian endometrioma and epithelial ovarian cancer. *J Ovarian Res*. 2013;6:44.
35. O'Shannessy DJ, Somers EB, Palmer LM, et al. Serum folate receptor alpha, mesothelin and megakaryocyte potentiating factor in ovarian cancer: association to disease stage and grade and comparison to CA125 and HE4. *J Ovarian Res*. 2013;6:29.
36. Nguyen L, Cardenas-Goicoechea SJ, Gordon P, et al. Biomarkers for early detection of ovarian cancer. *Womens Health*. 2013;9: 171–185.
37. Eisenhauer EA, Therasse P, Bogaerts J, et al. New response evaluation criteria in solid tumours: revised RECIST guideline (version 1.1). *Eur J Cancer*. 2009;45:228–247.
38. Kasten BB, Azure MT, Schoeb TR, et al. Imaging, biodistribution, and toxicology evaluation of (212)Pb-TCMC-trastuzumab in nonhuman primates. *Nucl Med Biol*. 2016;43:391–396.
39. Cramer DW, Bast RC Jr, Berg CD, et al. Ovarian cancer biomarker performance in prostate, lung, colorectal, and ovarian cancer screening trial specimens. *Cancer Prev Res*. 2011;4:365–374.
40. Dikmen ZG, Colak A, Dogan P, et al. Diagnostic performances of CA125, HE4, and ROMA index in ovarian cancer. *Eur J Gynaecol Oncol*. 2015;36:457–462.
41. Salmena L, Shaw P, Fans I, et al. Prognostic value of INPP4B protein immunohistochemistry in ovarian cancer. *Eur J Gynaecol Oncol*. 2015;36:260–267.
42. Seagle BL, Eng KH, Dandapani M, et al. Survival of patients with structurally-grouped TP53 mutations in ovarian and breast cancers. *Oncotarget*. 2015;6:18641–18652.
43. Tamir A, Jag U, Sarojini S, et al. Kallikrein family proteases KLK6 and KLK7 are potential early detection and diagnostic biomarkers for serous and papillary serous ovarian cancer subtypes. *J Ovarian Res*. 2014;7:109.
44. Wu Y, Lu M, Zhou Q. Kallikrein expression as a prognostic factor in ovarian cancer: a systematic review and meta-analysis. *J BUON*. 2015;20:855–861.
45. Urieli-Shoval S, Finci-Yeheskel Z, Dishon S, et al. Expression of serum amyloid a in human ovarian epithelial tumors: implication for a role in ovarian tumorigenesis. *J Histochem Cytochem*. 2010; 58:1015–1023.
46. Wilailak S, Chan KK, Chen CA, et al. Distinguishing benign from malignant pelvic mass utilizing an algorithm with HE4, menopausal status, and ultrasound findings. *J Gynecol Oncol*. 2015;26: 46–53.
47. Karlsen MA, Sandhu N, Hogdall C, et al. Evaluation of HE4, CA125, risk of ovarian malignancy algorithm (ROMA) and risk of malignancy index (RMI) as diagnostic tools of epithelial ovarian cancer in patients with a pelvic mass. *Gynecol Oncol*. 2012;127: 379–383.
48. Johnston WW, Szpak CA, Lottich SC, et al. Use of a monoclonal antibody (B72.3) as a novel immunohistochemical adjunct for the diagnosis of carcinomas in fine needle aspiration biopsy specimens. *Hum Pathol*. 1986;17:501–513.
49. Thor A, Gorstein F, Ohuchi N, et al. Tumor-associated glycoprotein (TAG-72) in ovarian carcinomas defined by monoclonal antibody B72.3. *J Natl Cancer Inst*. 1986;76:995–1006.
50. Thor A, Ohuchi N, Szpak CA, et al. Distribution of oncofetal antigen tumor-associated glycoprotein-72 defined by monoclonal antibody B72.3. *Cancer Res*. 1986;46:3118–3124.

